ISSN 2658-3518

LIMNOLOGY & FRESHWATER BIOLOGY

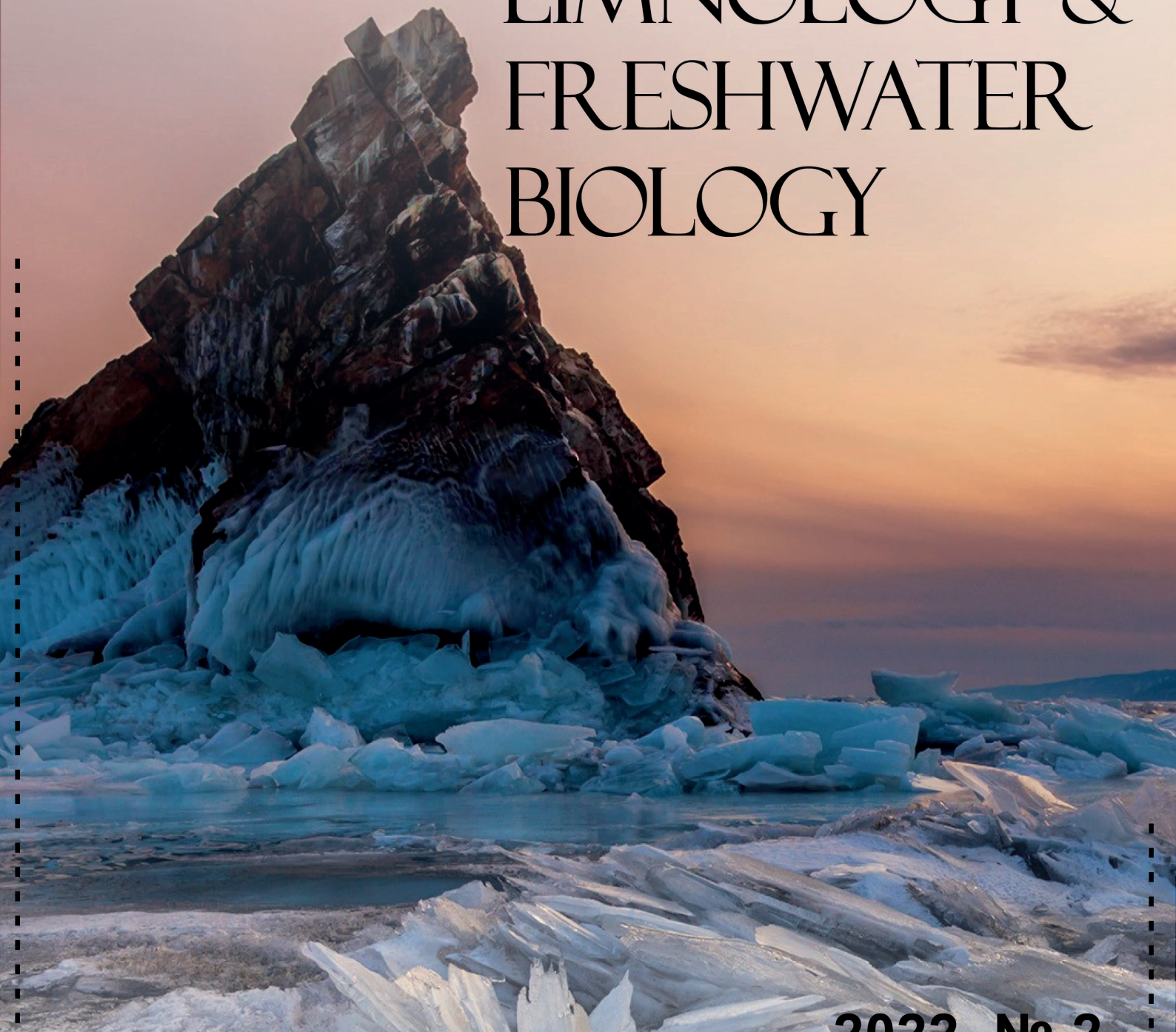

2022, № 2

> abiotic and biotic water components;
> ecosystem-level studies;
> systematics and aquatic ecology;
> paleolimnology and environmental histories;
> laboratory experiments and modeling

Limnology and Freshwater Biology 2022 (2): 1217-1228 DOI:10.31951/2658-3518-2022-A-2-1217

Original Article

ISSN 2658-3518
LIMNOLOGY FRESHWATER BIOLOGY
www.limnolfwbiol.com

Spatial and temporal variations of physical-chemical parameters of the Akor River in Ikwuano local government of Abia state, Nigeria

Odo S.N.[1,*], Odo M.K.[2], Anyanwu E.D.[3], Ikechukwu P.I.[1]

[1] Department of Fisheries and Aquatic Resources Management, Michael Okpara University of Agriculture, Umudike, Nigeria
[2] Department of Environmental Management and Toxicology. Michael Okpara University of Agriculture, Umudike, Nigeria
[3] Department of Zoology and Environmental Biology, Michael Okpara University of Agriculture, Umudike, Nigeria

ABSTRACT. Physical-chemical parameters of the Akor River were investigated. The river water was sampled for seven months (February –August) in 2019 and analysed following standard procedures and protocols. The results revealed that there were no significant differences ($P > 0.05$) among all the investigated physical-chemical parameters across stations. Mean values of all the investigated physical-chemical parameters were within Federal Ministry of Environment set standards (2011) except for chemical oxygen demand and pH. Spatiotemporal results revealed that turbidity, total suspended solids, total dissolved solids, and the major cations (Na^+, K^+, Ca^{2+}, and Mg^{2+}) as well as the major anions (PO_4^{3-}, NO_3^- and SO_4^{2-}), were high during the rainy season months, but water temperature, pH, dissolved oxygen, and biochemical oxygen demand were higher during the dry season months. The percentage of Na^+ contents ranged from 15.85 to 16.39%, indicating that Akor River has excellent irrigation water quality. The Nemerow pollution index varied from 0.59 to 0.63, also indicating that the river water is of good quality. The water quality index results varied from 52.70 to 54.50%, indicating that Akor River has a good water quality status. The result of water pollution index revealed that Akor River status is excellent and capable of sustaining biodiversity as well as crop irrigation.

Keywords: spatiotemporal variations, physical-chemical parameters, surface water, water pollution index

1. Introduction

Water is one of the most essential resources for the survival of man and other living organisms. The capacity of water source, especially surface water body, to sustain its potential depends on human activities within and around it. Surface water bodies have been significantly affected by anthropogenic activities, causing water quality deterioration, decreasing water availability and reducing the carrying capacity of aquatic life (Wang et al., 2012; Zhang et al., 2015; Harding et al., 2019).

Surface water body polluted by anthropogenic activities becomes less suitable or unfit for drinking, domestic uses, crop irrigation, fisheries, or other purposes. Continually drinking water from a polluted water body could cause human population to suffer from different waterborne diseases. The availability of good quality water is an indispensable feature for preventing diseases and improving quality of life of people, who always depend on surface water bodies for drinking water and other purposes.

Water bodies supplying drinking water for people have to be of good quality parameters. Assessment of water quality is very important to evaluate the "health" of ecosystems, to control environmental pollution and, hence, to maintain human safety (Anyanwu and Umeham, 2020). Nowadays, water quality is assessed by measuring environmental variables and by freshwater organisms in order to determine the environmental status of the ecosystem (Anyanwu et al., 2019).

Changes in the river water quality due to anthropogenic activities are a cause of growing concern and require monitoring of the surface waters (Parvez et al., 2019). Research has revealed that most of the freshwater bodies globally are increasingly polluted as a result of anthropogenic activities, thus affecting the derivable ecosystem services (Gupta et al., 2005; Anyanwu, 2012; Goldschmidt, 2016; Amah-Jerry et al., 2017). Many studies discussed physical-chemical parameters of rivers around the world (Table 1), but none of them was carried out on the Akor River so far.

The Akor River is subjected to several human activities, including sand mining, lumbering, water

*Corresponding author.
E-mail address: odofavour4real@gmail.com (S.N. Odo)

Received: December 29, 2021; ***Accepted:*** April 18, 2022;
Available online: May 25, 2022

irrigation of farms and nursery, application of fertilizers and pesticides, extraction of water for drinking and other domestic uses: washing, swimming and food processing. Some of them take place within the watersheds, which could negatively affect the water quality as well as derivable ecosystem services through direct or indirect impacts and discharges or runoffs. Thus, the present study assessed spatial and temporal variation of chemical parameters in the Akor River in Ikwuano Local Government of Abia State.

2. Materials and methods

2.1. Description of study area

The Akor River takes its source from Bende in Abia North and passes through many communities (including Nkanu Nta, Obuoru, and Itunta) before discharging into the Cross River at Itunta. The stretch of the Akor River studied is between Obuoru and Itunta in Ikwuano L.G.A, Abia State; about 2.38 km in length. It lies between latitude of 5°26.854' and 5°28.031'N and longitude of 7°37.860' and 7°38.838'E. The major activities in and around the Akor River are palm oil production, cocoa farming, sand mining, lumbering, rice and cocoa nurseries, rice, cocoa, cassava and vegetable farming as well as others, including bathing, swimming, washing, fishing, and extraction of water for drinking and other domestic uses. For the purpose of this study, three stations were selected based on accessibility and anthropogenic activities.

Station 1 was upstream, located in Obuoru, Ibere (Fig.1). The observed human activities are laundry, swimming, fishing, extraction of drinking water, sand mining, washing of bread fruit, and lumbering. The substrate was sand, and the flow velocity was moderate.

Station 2 was located in Itunta near the bridge about 1.39 km downstream of Station 1 (Fig.1). There was a less active sand mining site, cocoa and rice nurseries and large expanse of cocoa farms. Other activities were laundry, fishing, swimming, and extraction of drinking water. It was open, vegetated and wadeable with relatively high velocity, and the substrate was also sand.

Station 3 was also located in Itunta Ibere about 0.99 km (990 m) downstream of Station 2 (Fig.1). Sand mining, vegetable cropping and cocoa farming activities were observed at this station. It was open vegetated with relatively high velocity and sandy substrate.

2.2. Water sampling

Sampling for water parameters was carried out at the three stations at monthly intervals between February and August 2019. The sampling period covered dry season, onset of rain and peak of rainy season. The collected water samples were taken with sterile one (1 litre) plastic containers. The containers were rinsed three times with the water samples to be collected at the site before collection was made.

Water temperature and pH were measured by digital pH meter/ thermometer (Hach EC 20),

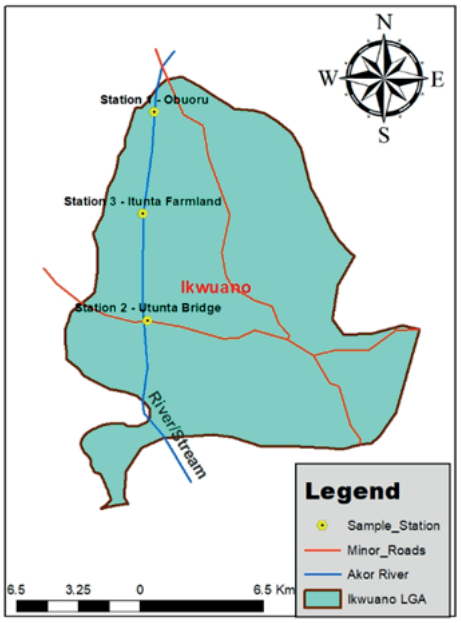

Fig.1. Map of study area with sampling points.

electrical conductivity was measured by Hach CO 150 conductivity meter. To determine total dissolved solids (TDS) and total suspended solids (TSS) content, gravimetric method was used. Turbidity was determined by Jenway 6035 Portable Turbidimeter. To determine dissolved oxygen (DO) content and biochemical oxygen demand (BOD), Winkler method with azide modification was used. Chemical oxygen demand (COD) was determined using open reflux method. NO_3^- was analyzed using Hach DR 1900 spectrophotometer. SO_4^{2-} was determined by turbidimetric method. PO_4^{3-} was determined by the stannous chloride method. K^+ was determined by flame photometry while other major cations (Na^+, Ca^{2+}, and Mg^{2+}) were analyzed using atomic emission spectroscopy.

2.3. Water pollution index

Pollution index of the Akor River was evaluated using Nemerow pollution index (NPI) as described by Anyanwu and Umeham (2020):

$$NPI = \sqrt{\frac{\left(\frac{C_i}{L_i}\right)_M^2 + \left(\frac{C_i}{L_i}\right)_R^2}{2}} \quad (1),$$

where NPI is the pollution index for a specified water quality purpose; C_i is measured water quality parameter; L_i is the standard water quality parameter for each parameter of specified water quality purpose; $\left(\frac{C_i}{L_i}\right)_M$ is C_i/L_i maximum, and $\left(\frac{C_i}{L_i}\right)_R$ is C_i/L_i average.

The percentage of sodium (%Na) was evaluated as described by Al-Othman (2019) using:

$$\%Na = 100 \cdot \frac{Na}{(Ca + Mg + K + Na)} \quad (2),$$

where Ca is Ca^{2+} concentration; Mg is Mg^{2+} concentration; Na is Na^+ concentration, and K is K^+ concentration. The quantities of all ions are expressed in mg/L.

The water quality index (WQI) was calculated as described by Anyanwu and Umeham (2020) using:

$$WQI = \frac{\sum q_i \cdot W_i}{\sum W_i} \quad (3).$$

The quality rating scale for each parameter q_i was calculated using the following expression:

$$q_i = 100 \cdot \frac{V_n}{V_i} \quad (4),$$

where V_n is the actual amount of nth parameter, and V_i is the standard (Table 2).

Relative weight (W_i) was calculated by a value inversely proportional to the standard of the corresponding parameter:

$$W_i = \frac{1}{V_i} \quad (5).$$

2.4. Data analysis

One-way analysis of variance (ANOVA) followed by Tukey Pairwise test (DMRT) was used to determine the differences between the sampling sites and months using SPSS IBM (Version 20 for Windows) statistical package at $P < 0.05$ level of significance.

Table 1. Physical-chemical characteristics of some selected surface water bodies (rivers).

Parameter	Water body	Range	Reference
T, °C			
	Aba River, Nigeria	23.5 - 29.3	Amah-Jerry et al. (2017)
	Ossah River, Nigeria	21.0 - 28.0	Anyanwu et al. (2019)
	Obot Okoho Stream, Nassarawa	25.4 - 27.2	Eni et al. (2014)
	Ogba River, Benin City	20.0 - 25.6	Anyanwu (2012)
	Gboko stream	30.2 - 30.8	Ubwa et al. (2013)
	Oshunkaye stream in Ibadan	31.0 - 34.0	Osibanjo and Adie (2007)
pH			
	South eastern River	4.6 - 6.3	Anyanwu and Ukaegbu (2019)
	Aba river	5.0 - 7.3	Amah-Jerry et al. (2017)
	Water sources in Ife	6.5 - 8.9	Oluyemi et al. (2010)
	Saba River, Osogbo	7.2 -7.6	Yusuf et al. (2017)
EC, µS/CM			
	Ogba River, Benin City, Nigeria	23.3 - 116.5	Anyanwu (2012)
	Athi River in Machakos, Kenya	12.0 – 1580.0	Ratemo (2018)
	Ole Stream Abeokuta, Ogun state	188.4 - 321.6	Adeosun et al. (2016)
DO, mg/L			
	River	3.2 - 6.4	Anyanwu et al. (2019)
	Ossah River, Nigeria	2.7 - 8.8	Amah-Jerry et al. (2017)
BOD, mg/L			
	Ogba River, Benin City, Nigeria	1.7 - 4.8	Anyanwu (2012)
	South eastern River	1.5 - 4.2	Anyanwu and Ukaegbu (2019)
COD, mg /L			
	Ganga River	6.5 - 8.5	Matta et al. (2018)
	Saba River, Osogbo	14.9 - 31.5	Yusuf et al. (2017)
	Aba River	2.3 - 7.0	Amah-Jerry et al. (2017)
	Illo River, Ota	425.0 - 1675	Omole and Longe (2008)
PO_4^{3-}, mg /L			
	Saba River, Osogbo	1.9 and 3.8	Yusuf et al. (2017)
	Aba River	2.3 and 79.8	Amah-Jerry et al. (2017)
SO_4^{2-}, mg /L			
	Ogba River, Benin City	0.60 and 6.39	Anyanwu (2012)
	Ekerekana and Buguma Creeks, Niger Delta	7.10 and 24.64	Makinde et al. (2015)
	Aba river	30.1 - 120	Amah-Jerry et al. (2017)
	Ikwu River Umuahia Abia State	0.3 and 1.3	Anyanwu and Emeka (2019)
Ca^{2+}, mg/L			
	Ogba River, Benin City	9.6 and 19.2	Anyanwu (2012)
	Ikpoba River	4.8 and 25.0	Ogbeibu and Edutie (2002)
	Utor River	0.4 and 19.2	Ogbeibu and Edutie (2002)

Note. T – temperature; EC - electrical conductivity; DO – dissolved oxygen; BOD – biochemical oxygen demand; COD - chemical oxygen demand.

3. Results

The results of the physical-chemical parameters of the Akor River are summarized in Table 2.

3.1. Physical-chemical parameters

Water temperature

The spatial and temporal variations of surface water temperatures are shown in figure 2. The temperature values recorded ranged between 24.0 and 29.0°C (Table 2). The lowest temperature value (24.0°C) was recorded at Station 3 in July 2019, while the highest temperature (29.0°C) was recorded at Station 2 in February 2019 (Fig. 2). The lowest mean value was recorded at Station 1, while the highest one was recorded at Station 2 (Table 2). There was no significant difference ($P > 0.05$) in temperature values among the stations when ANOVA was applied.

Turbidity

The spatial and temporal variations of turbidity values are shown in figure 3. Turbidity values ranged between 0.2 and 1.5 NTU (Table 2). The lowest values were recorded at Station 1 and Station 2 during the dry season in March 2019, while the highest values were recorded at Station 1 and Station 3 during the onset of rains in May 2019. Turbidity shows a clear trend: the turbidity increased with an increase in rains between March and May 2019 and gradually decreased afterwards from May to August (Fig. 3).

One-way analysis of variance (ANOVA) test employed to ascertain whether there are statistical differences in the values recorded at all stations showed that there were no significant differences in turbidity ($P > 0.05$) at all stations. The highest mean value was recorded at Station 1, while the lowest one was recorded at Station 2. All recorded values were within the acceptable limit of 5 NTU set by FMEnv (2011).

pH

The spatial and temporal variations of pH are shown in figure 4. The values were acidic, with a range of 4.6 to 6.6 mg/L (Table 2). The lowest and highest values were recorded at Station 1 in May and February 2019, respectively. All pH values were outside the acceptable limit of 6.5 to 8.5 set by FMEnv (2011), except for 6.5 and 6.6 recorded in March 2019 (Station 2) and February 2019 (Station 1), respectively. All mean values were also acidic and outside the acceptable limits. The lowest mean value was recorded at Station 2, while the highest ones were recorded at Stations 1 and 3. There was no significant difference ($P > 0.05$) in the pH values across all the stations.

Electrical conductivity (EC)

The electrical conductivity (EC) values ranged between 32.6 and 128.4 µS/CM (Fig. 5). All values were low and within the acceptable limits set by FMEnv (2011), though relatively high values were recorded in May 2019 at all stations. The mean values increased spatially from Station 1 to Station 3 (Table 2). There was no significant difference ($P > 0.05$) in the EC values across all the stations.

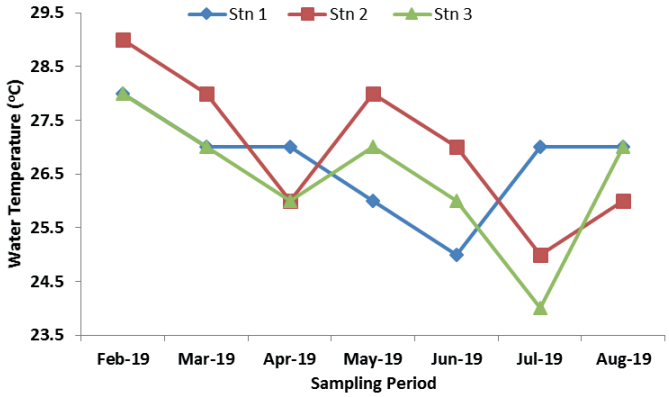

Fig.2. Spatial and temporal variations of temperature at the study stations of the Akor River.

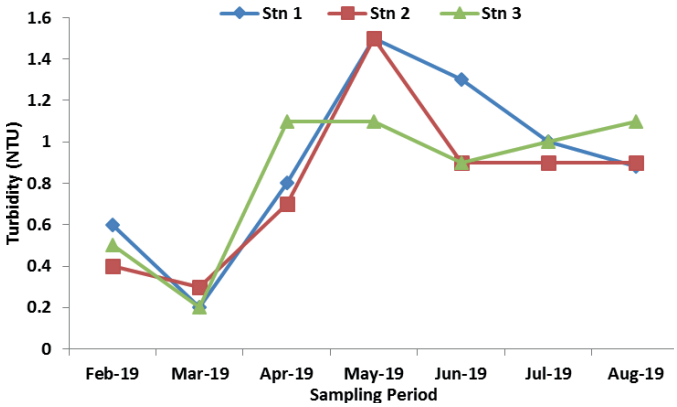

Fig.3. Spatial and temporal variations of turbidity at the study stations of the Akor River.

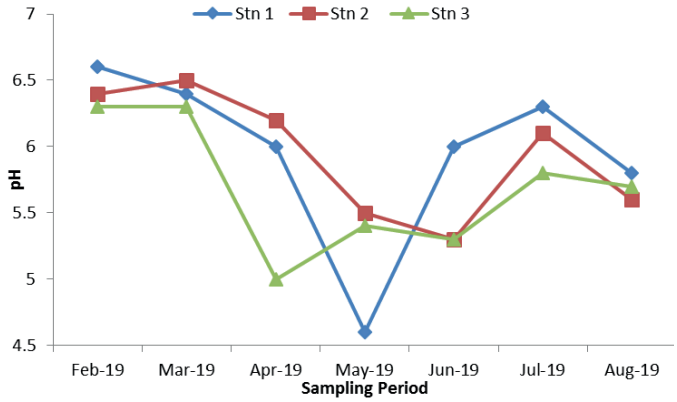

Fig.4. Spatial and temporal variations of pH at the study stations of the Akor River.

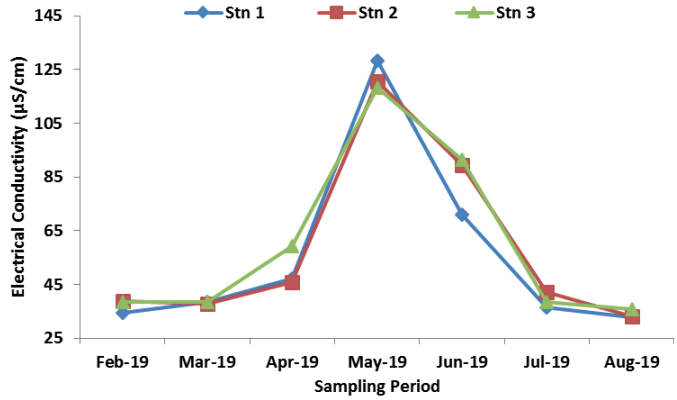

Fig.5. Spatial and temporal variations of EC at the study stations of the Akor River.

Table 2. Summary of physical-chemical parameters of the Akor River (with range given in parentheses).

Parameter	Station 1	Station 2	Station 3	P-value	FMEnv., 2011
T, °C	26 ± 0.36 (25-28)	27 ± 0.53 (25- 29)	26.42 ± 0.48 (24 -28)	P > 0.05	30
Turbidity, NTU	0.90 ± 0.16 (0.2 -1.5)	0.80 ± 0.15 (0.3 -1.5)	0.85 ± 0.14 (0.2 -1.1)	P > 0.05	5
pH	5.96 ± 0.25 (4.6 - 6.6)	5.94 ± 0.18 (5.3 - 6.5)	5.96 ± 0.18 (5.0 - 6.3)	P > 0.05	8.5
EC, µS/cm	55.56 ± 13.3 (32.6-128.4)	58.29 ± 12.62 (33.2 -120.5)	60.00 ± 12.3 (35.0 - 118.3)	P > 0.05	1000
TDS, mg/L	26.14 ± 7.04 (13.3 -64.4)	28.83 ± 6.52 (13.3 -60.4)	29.37 ± 6.41 (13.6 -59.2)	P > 0.05	500
TSS, mg/L	2.10 ± 0.41 (0.6-4.2)	2.14 ± 0.38 (0.9-4.0)	2.31 ± 0.41 (0.7 -3.7)	P > 0.05	0.25
DO, mg/L	4.91 ± 0.82 (4.3 -6.8)	4.34 ± 0.80 (3.4 -6.4)	4.37 ± 0.70 (4.0 -6.3)	P > 0.05	6
BOD, mg/L	1.50 ± 0.18 (1.0 -2.4)	1.61 ± 0.25 (1.2 - 2.1)	1.69 ± 0.14 (1.2 - 2.3)	P > 0.05	3
COD, mg/L	191.93 ± 58.1 (41.2-480.1)	175.03 ± 63.5 (28.8-416.00)	180.86 ± 68.8 (31.2-491.00)	P > 0.05	30
SO_4^{2-}, mg /L	0.30 ± 0.10 (0.09-0.85)	0.34 ± 0.10 (0.09 -0.75)	0.35 ± 0.10 (0.10-0.73)	P > 0.05	100
NO_3^-, mg/L	0.82 ± 0.23 (0.30-2.15)	0.84 ± 0.20 (0.24-1.88)	0.84 ± 0.18 (0.27-1.75)	P > 0.05	9.1
PO_4^{3-}, mg /L	1.29 ± 0.35 (0.50-3.12)	1.32 ± 0.32 (0.36-2.85)	1.29 ± 0.31 (0.50-2.71)	P > 0.05	3.5
Na^+, mg/L	0.81 ± 0.23 (0.22-2.1)	0.87 ± 0.22 (0.37-1.57)	0.98 ± 0.24 (0.27-1.88)	P > 0.05	120
K^+, mg/L	0.36 ± 0.10 (0.08-0.91)	0.30 ± 0.08 (0.13-0.73	0.38 ± 0.08 (0.11-0.64)	P > 0.05	50
Ca^{2+}, mg/L	2.56 ± 0.70 (0.88-6.44	2.59 ± 0.63 (0.72-5.12)	2.71 ± 0.58 (0.98-4.83)	P > 0.05	180
Mg^{2+}, mg/L	1.49 ± 0.48 (0.66-4.32)	1.73 ± 0.48 (0.51-4.11)	1.91 ± 0.46 (0.66-3.75)	P > 0.05	40
% Na	15.59	15.85	16.39		
NPI	0.63	0.59	0.61		
WQI	53.42	52.70	54.50		

Note. Column 6 (FMEnv., 2011) – upper permissible limits of physical-chemical parameters given by Federal ministry of environment (2011); T – water temperature; EC - electrical conductivity; TDS - total dissolved solids; TSS - total suspended solids; DO – dissolved oxygen; BOD – biochemical oxygen demand; COD - chemical oxygen demand; % Na – sodium percentage; NPI - Nemerow pollution index; WQI - water quality index.

Dissolved oxygen (DO)

The spatiotemporal variations of dissolved oxygen are presented in figure 6. The values ranged between 3.4 and 6.8 mg/L (Table 2). The lowest value was recorded at Station 2 (July 2019), while the highest one was recorded at Station 1 (May 2019). Most of the values recorded were below the acceptable limit (6 mg/L) set by FMEnv (2011) though values recorded at Station 1 (May and June 2019), Station 2 (April 2019) and Station 3 (February 2019) were above the limit (Fig. 6). The mean values decreased spatially with no significant difference (P > 0.05) between the stations.

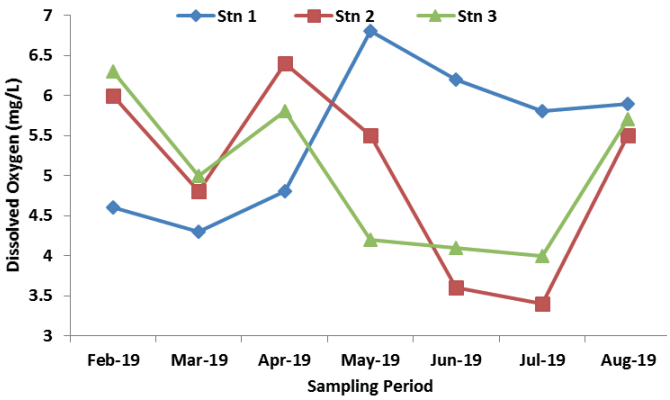

Fig.6. Spatial and temporal variations of DO at the study stations of the Akor River.

Biochemical oxygen demand (BOD)

The spatiotemporal variations of BOD are presented in figure 7. The values of BOD ranged from 1.0 to 2.4 mg/L (Table 2), the spatial and temporal variations of which are shown in figure 7. The lowest and highest values were recorded at Station 1 in February and May 2019, respectively. All BOD values recorded were below 3.0 mg/L set by FMEnv (2011). The mean values increased spatially, though there was no significant difference ($P > 0.05$) across the stations.

Total dissolved solids (TDS)

The spatial and temporal variations of total dissolved solids (TDS) are shown in figure 8. The TDS values ranged from13.3 to 64.4 mg/L (Table 2). All values were within the acceptable limit set by FMEnv (2011). The lowest values were recorded at Station 1 (July 2019) and Station 2 (February 2019), while the highest one was recorded in May 2019 at Station 1. TDS followed the same trend as electrical conductivity (EC). The mean values also increased spatially, though there was no significant difference ($P > 0.05$) across the stations.

Total suspended solids (TSS)

The spatial and temporal variations of total suspended solid (TSS) are shown in figure 9. The TSS values ranged between 0.6 and 4.2 mg/L (Table 2). The lowest and highest values were recorded at Station 1 in March 2019 and May 2019, respectively. All values exceeded the acceptable limit (0.25 mg/L) set by FMEnv (2011). TSS followed the same trend as turbidity. The mean values also increased spatially, though there was no significant difference ($P > 0.05$) across the stations.

Chemical oxygen demand (COD)

The spatial and temporal variations of chemical oxygen demand (COD) are shown in figure 10. The values ranged between 28.8 and 491.0 mg/L (Table 2). The lowest values were recorded at Station 2 (March and June 2019), while the highest one was recorded at Station 3 (April 2019). All values exceeded the acceptable limit (30 mg/L) set by FMEnv (2011), except for 28.8 mg/L recorded at station 2 in March and June 2019 (Fig. 10). The highest mean value was recorded at Station 1, while the lowest one was recorded at Station 2. There was no significant difference ($P > 0.05$) in COD across the stations.

SO_4^{2-}

The spatial and temporal variations of SO_4^{2-} are shown in figure 11. The values ranged between 0.09 and 0.85 mg/L (Table 2). The lowest values were recorded at Station 1 and Station 2 (February and March 2019, respectively), while the highest value was recorded at Station 1 (May 2019). All values were lower than acceptable limit (100 mg/L) set by FMEnv (2011) at all stations in 2019 (Fig. 11). The highest mean value was recorded at Station 2, while the lowest one was recorded at Station 3. There was no significant difference ($P > 0.05$) in SO_4^{2-} across the stations.

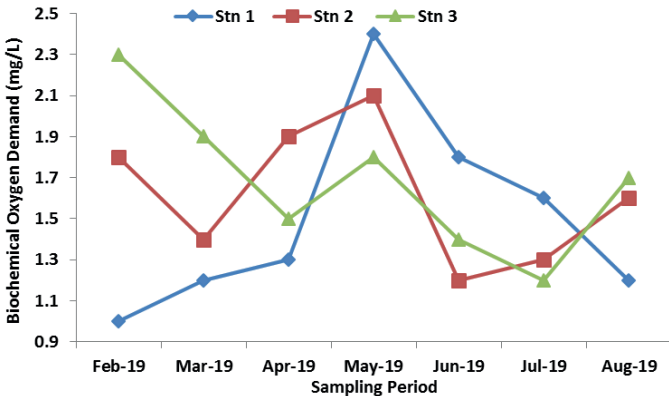

Fig.7. Spatial and temporal variations of BOD at the study stations of the Akor River.

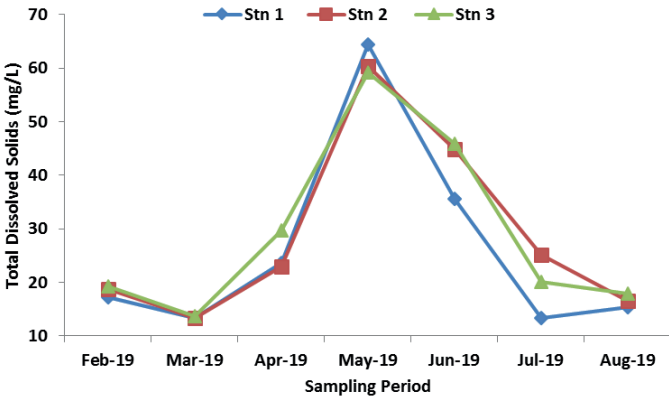

Fig.8. Spatial and temporal variations of TDS at the study stations of the Akor River.

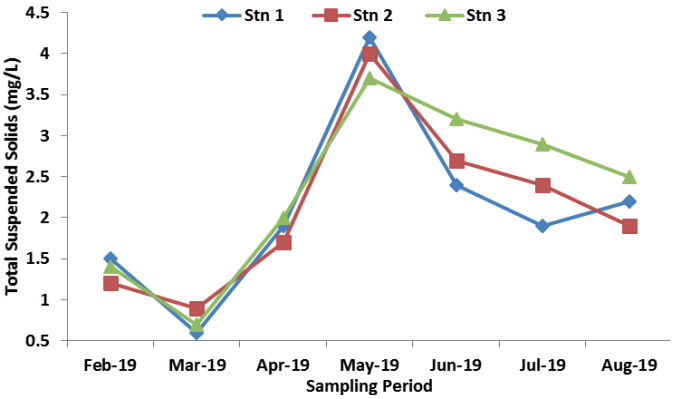

Fig.9. Spatial and temporal variations of TSS at the study stations of the Akor River.

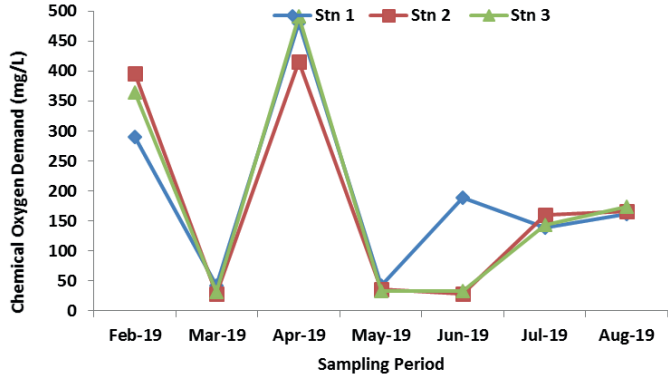

Fig.10. Spatial and temporal variations of COD at the study stations of the Akor River.

PO_4^{3-}

The spatial and temporal variations of PO_4^{3-} are shown in figure 12. The values ranged between 0.36 and 1.12 mg/L (Table 2). The lowest values were recorded at Station 2 (March 2019), while the highest value was recorded at Station 1 (May 2019). All values were lower than acceptable limit (3.5 mg/L) set by FMEnv (2011) at all stations in 2019 (Fig. 12). There was no significant difference ($P > 0.05$) in PO_4^{3-} across the stations.

NO_3^-

The spatial and temporal variations of NO_3^- are shown in figure 13. The NO_3^- values ranged between 0.24 mg/L and 2.15 mg/L. (Table 2). All values were lower than acceptable limit (9.1 mg/L) set by FMEnv (2011). The lowest values were recorded at Station 1 (March 2019), while the highest value was recorded at Station 1 in May 2019. The mean values also increased spatially, though there was no significant difference ($P > 0.05$) across the stations.

Na^+

Spatial and temporal variation of Na^+ values was shown in figure 14. The values ranged between 0.22 and 2.1 mg/L (Table 2). All the values were much lower than acceptable limit (120 mg/L) set by FMEnv. (2011). Both lowest and highest values were recorded at Station 1 in March 2019 and May 2019, respectively. The mean values had no significant difference ($P > 0.05$) across the stations.

K^+

The spatial and temporal variations of K^+ are shown in figure 15. The values ranged from 0.08 to 0.91 mg/L (Table 2). The lowest and highest values were recorded at Station 1 in February and May 2019, respectively. All K^+ values were lower than the acceptable limit of 50 set by FMEnv (2011). There was no significant difference ($P > 0.05$) in the K values across all stations.

Ca^{2+}

The concentration of Ca^{2+} measured at the three stations during this study period ranged from 0.72 to 6.44 mg/L. The lowest and highest Ca^{2+} concentrations were recorded at Station 1 in February and at Station 2 in May, respectively. Results of Ca^{2+} contents indicated no significant difference across the three stations. The spatial variation of Ca^{2+} at Station 1 revealed gradual increments between February and April, then sharp increments in May, and afterward, it gradually decreased until the end of this study period. Spatial variation at Station 3 followed the same trend with no variations between February and March (Fig. 16). At Station 2, the trend decreased from February to March but increased between March and May and then decreased.

Mg^{2+}

The concentrations of Mg^{2+} ranged between 0.51 and 4.32 mg/L. The highest concentration of Mg^{2+} was recorded in May 2019 across the three stations, whereas the lowest concentration was recorded at Station 1 in February 2019, though Stations 2 and 3 recorded their lowest concentrations

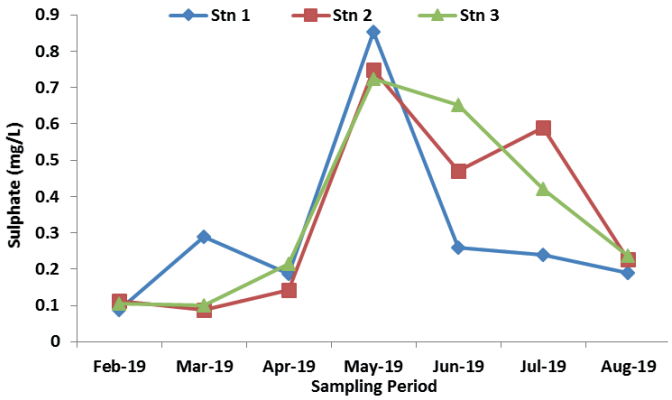

Fig.11. Spatial and temporal variations of SO_4^{2-} at the study stations of the Akor River.

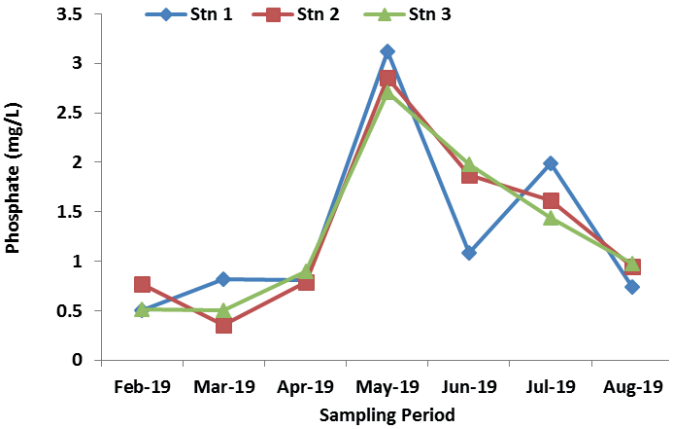

Fig.12. Spatial and temporal variations of PO_4^{3-} at the study stations of the Akor River.

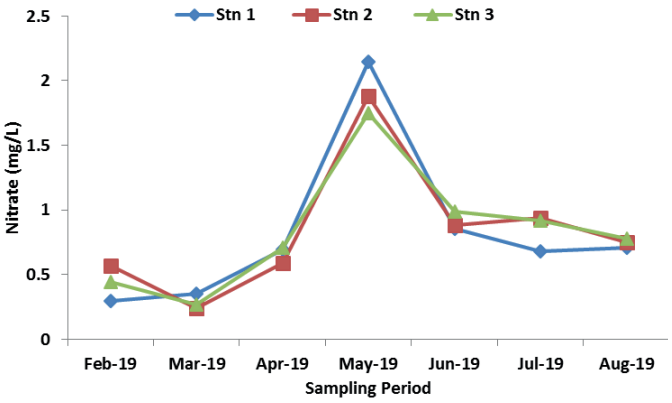

Fig.13. Spatial and temporal variations of NO_3^- at the study stations of the Akor River.

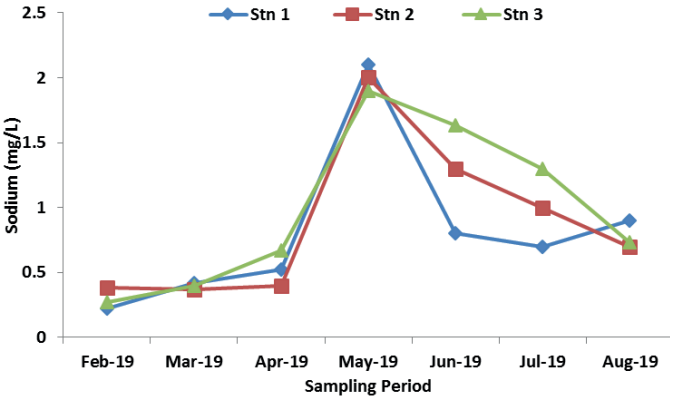

Fig.14. Spatial and temporal variations of Na^+ at the study stations of the Akor River.

in March 2019. No significant difference ($P > 0.05$) was recorded among the stations. The spatial variation of Mg^{2+} concentration followed the same trend as Ca^{2+}. At Station 1, there were gradual increments between February and May, then there was a monthly decreased throughout the study period. At the same time, at Station 2 and Station 3, the trend revealed a decrease between February and March followed by a gradual increase between March and April, then there was a drastic increase in May (onset of rain) and afterwards a monthly decrease throughout the study period (Fig. 17).

3.2. Water pollution index

The percentage of Na^{+} ranged from 15.85 to 16.39%, indicating that Akor River has excellent irrigation water quality. The highest value was recorded at Station 3 (July), whereas the lowest value was observed at Station1 (February). The Nemerow pollution index varied from 0.59 to 0.63, which also indicated that the water in the river is of good quality. The water quality index results varied from 52.70 to 54.50%, indicating that the Akor River has good water quality status. The result of water pollution index revealed that the Akor River status is excellent and capable of sustaining biodiversity as well as crop irrigation.

4. Discussion

4.1. Physical-chemical parameters

This study compared the impact of anthropogenic activities on water quality of the Akor River, Ikwuano, Abia state, Nigeria. There are some marked variations in the physical-chemical parameters observed from the sampling stations and the seasons on the river. The range of surface water temperature for the river correlated well with the ranges recorded for other southeast surface river waters (Amah-Jerry et al., 2017; Anyanwu et al., 2019; Anyanwu and Ukaegbu, 2019). Both micro- and macro-aquatic organisms depend on certain temperature range for optimal growth and survival. The higher surface water temperature of the river during the dry season could be attributed to climate variability such as air temperatures and associated sunshine. Many studies recorded surface water temperatures within or slightly lower than the range obtained in this study.

Turbidity is a resultant accumulation of materials such as organic and inorganic materials, plankton and other microscopic organisms, including mud (Effendi et al., 2015). The mean values of turbidity during this study period were higher than the mean values (1.98 ± 0.91 NTU) obtained by Anyanwu and Ukaegbu (2019) for the Ossah River, southeastern Nigerian river. In the same line, Anyanwu (2012) reported higher values of turbidity for the Ogba River, Benin City, Nigeria, than the results obtained in this study. The results revealed relatively higher turbidity values during the rainy season. This may be attributed

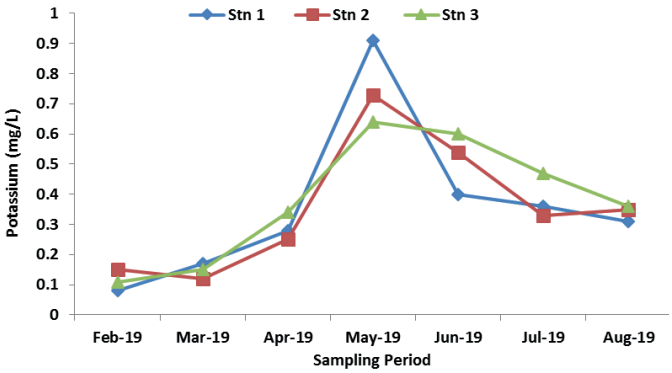

Fig.15. Spatial and temporal variations of K^{+} at the study stations of the Akor River.

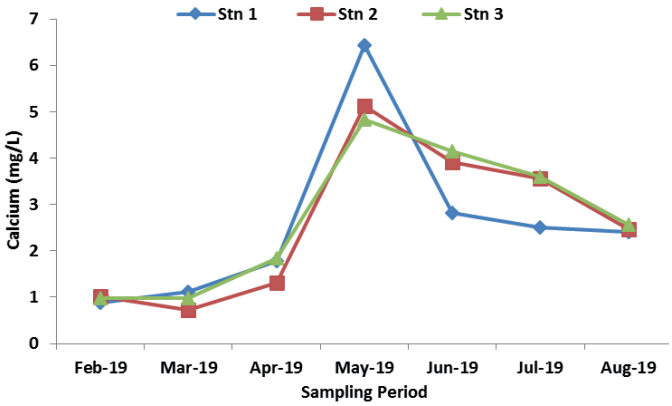

Fig.16. Spatial and temporal variations of Ca^{2+} at the study stations of the Akor River.

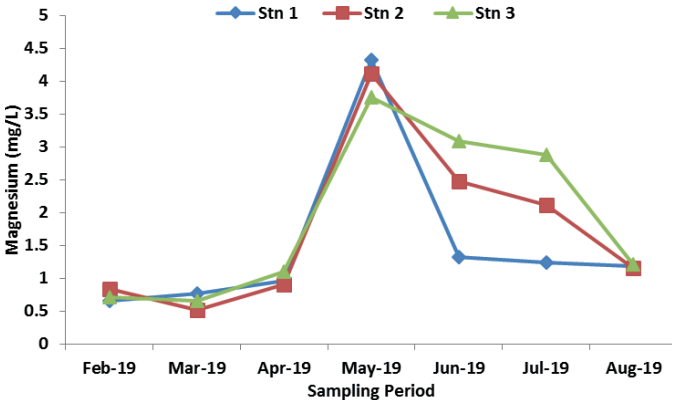

Fig.17. Spatial and temporal variations of Mg^{2+} at the study stations of the Akor River.

to emptying of suspended solids loads into the river via runoffs. The variation patterns obtained across all the sampling stations on both rivers could be attributable to the degree of anthropogenic activities in and around the river.

The pH values obtained during this study were within acidic range and this is in line with results obtained by Anyanwu and Ukaegbu (2019) and Amah-Jerry et al. (2017) in Ossah River, Umuahia and Aba River, Aba, Southeast Nigeria. The pH values in this study were lower than the values obtained by Oluyemi et al. (2010) from the water sources in Ife North Local Government Area of Osun State and Yusuf et al. (2017) that recorded pH values ranging from nearly neutral to weakly alkaline in the Saba River, Osogbo, both in

Southwest Nigeria. Water pH determines the solubility and biological availability of chemical constituents such as nutrients and heavy metals in surface water. All pH values recorded were acidic and below the acceptable limit set by SON (2015). This could be attributed to geogenic influence. Studies have shown that rivers in the region are acidic (Okereke, 2014; Bobor and Umeh, 2019; Anyanwu and Umeham, 2020; Anyanwu et al., 2022). Geogenic low pH is usually a result of acid-generating rocks/soils and oxidation or reduction processes within the river (USEPA, 2022).

The results of conductivity indicate that anthropogenic activities had no noticeable impact on the river and equally showed that the river is a freshwater body. The EC values obtained during this study period were within or slightly higher than the values recorded for the Ogba River, Benin City, Nigeria by Anyanwu (2012). EC values were rather lower than the values recorded in the Ikwu River, Umuahia, Nigeria by Anyanwu et al. (2022). The low EC values obtained in this study corresponded to the low total dissolved solids, thus attributing the low EC to low TDS.

Dissolved oxygen is the quantity of oxygen dissolved in water, and it is essential to determine whether the water under study can support aquatic life (Joshua and Nazrul, 2015). The mean DO values recorded indicated that the Akor River can support aquatic life and is good for drinking. There is no public health implication of DO in drinking water but higher concentrations are associated with better water quality and taste (Omer, 2019). DO values were lower during the rainy season than the dry season and this could result from decomposition of eroded materials discharged into the river. The results of this study correlate with the findings of lower DO in rainy season (Amah-Jerry et al., 2017). The range of DO values recorded in this study is in line with the results obtained by Amah-Jerry et al. (2017) and Anyanwu et al. (2019). Similarly, the findings of this study corroborate the result of Adeosun et al. (2016) and Olalekan et al. (2012) that reported that DO values were higher in the rainy season than in the dry season in the Ole Stream of the Federal University of Agriculture, Abeokuta, and the Ogun River, respectively, both in Ogun state, Southwest Nigeria.

However, the result is not in line with Oribhabor et al. (2013) that reported that DO level was lower than in the rainy season in the Lower Cross River, Nigeria. The higher DO values recorded in the Akor River between March and June may be attributed to early rainfall that has led to the increase in water volume, turbulence and increased dissolution of oxygen at air-water interface.

Biochemical oxygen demand is one of the important parameters of water employed in determining the pollution load of freshwater bodies (Anyanwu et al., 2019). The results recorded indicate that the level of oxygen required by microorganisms for respiration in the water is lower than the required maximum standard of 3 mg/L. The BOD values obtained were in line with the study of Anyanwu (2012) on the Ogba River, Benin City, and of Anyanwu and Ukaegbu (2019) on the Ossah River, Umuahia, both in Southeast Nigeria. Anyanwu et al. (2019) recorded similar results for the Ossah River, Umuahia, Southeast Nigeria. However, the results of BOD recorded for most surface waters in Southwest Nigeria (Oluyemi et al., 2010) were higher than the values observed during this study period.

The BOD values recorded indicated that anthropogenic activities in and around the river had no significant impact on the quality of water and revealed that Akor River is a clean surface water body. The higher BOD recorded in the southwestern river than southeastern rivers, including the Akor, may be attributed to climate variables, anthropogenic activities and abundance of aquatic microflora and fauna within the region.

Total dissolved solids influence the aesthetic value of the water through altering the turbidity and limit water body from performing its ecosystem functions as a drinking water source and irrigation supply (Amanial, 2015; Titilawo et al., 2019). The TDS values obtained in the present study were the same or higher than those recorded by Amah-Jerry et al. (2017) on the Aba River, and Anyanwu et al. (2019) on the Ossah River, Umuahia, both in Southeast Nigeria. However, the results obtained in the present study were rather lower than in the study of Flura et al. (2016) in the Meghna River, Bangladesh, and Yusuf et al. (2017) on the Saba River, Osogbo, Nigeria. Similarly, higher values of TDS were recorded by Ewa et al. (2011) in the Omoku Creek and Makinde et al. (2015) in the Ekerekana and Buguma Creeks, both in the Niger delta, Nigeria.

Higher values of TDS recorded for the Akor River between April and June 2019 could probably be due to active various farming activities such as clearing, ploughing and ridge making in the farmlands around the river (Petlušová et al., 2019). Additionally, heavy runoffs as a result of early rainfall during these months may also have contributed immensely to these higher values.

Total suspended solids value is normally used as a potential index for drinking water contamination. The higher the TSS values, the higher likelihood of introduction of different diseases in the water body, which affect all living organisms, especially humans. Results of TSS obtained in the present study were lower than in the study of Amah-Jerry et al. (2017) on the Aba River, Southeast Nigeria. Similarly, the study of Danha et al. (2014) at discharging point and downstream of charging point recorded higher values than the present study. The higher TSS values obtained in the river between April and August could be attributed to high runoff as result of early rains that emptied debris and other suspended materials into the river.

Chemical oxygen demand values recorded were higher compared to 2.0-7.0 mg/L recorded in Aba River, Aba by Amah-Jerry et al. (2017) and 14.95-31.47 mg/L recorded in Saba River, Osogbo, Nigeria by Yusuf et al. (2017) but lower than 425.0-1675 mg/L recorded in Illo River, Ota, Nigeria by Omole and Longe (2008)

and 444.0-1508 mg/L recorded in a stream in Gboko, Nigeria by Ubwa et al. (2013). The highest COD values were recorded in April 2019 and declined afterwards; a trend observed by Yusuf et al. (2017). The COD values indicated that the Akor River was mildly polluted. The values of COD recorded in surface waters usually range from 20 mg/L or less in unpolluted waters to greater than 200 mg/L in effluent-receiving waterbodies (Chapman and Kimstach, 1996).

PO_4^{3-} value gives an indication of the degree of both nutrients and eutrophication of any aquatic system. Disposal of detergents, contaminated sewage and direct washing of clothes in water, as well as application of fertilizer, pesticides and other agrochemicals to crop plants, cause PO_4^{3-} contamination of water body (Anyanwu and Ukaegbu, 2019). PO_4^{3-} values recorded in this study were generally poorly compared to the data of Yusuf et al. (2017), Amah-Jerry et al. (2017), Osibanjo and Adie (2007), who studied the Nigerian rivers. However, the PO_4^{3-} values were within the range obtained by Anyanwu and Emeka (2019) for the Ikwu River and by Anyanwu and Ukaegbu (2019) in Umuahia Abia state, Southeast Nigeria. Similarly, the spatial variations and higher values during the rainy season in the Akor River may be attributed to early rains that empty both animal and human faeces into the river coupled with active farming activities such as the application of fertilizers, pesticides and other agrochemicals. The higher values of PO_4^{3-} in the Akor River could also be probably due to indiscriminating using of fertilizer and agrochemicals by rural cocoa and rice farmers.

NO_3^- values in natural surface waters are often less than 1 mg/L, but a water body under the influence of anthropogenic activities could have NO_3^- values up to 5 mg/L (Anyanwu and Ukaegbu, 2019). NO_3^- values above of 5 mg/L usually indicate anthropogenic activities or animal waste, or fertilizer pollution. The NO_3^- values in this study were within the values of natural river (< 1 mg/L), except for May when the values exceeded 1mg/L. The spatial and temporal variations recorded may be attributed to the application of nitrogen containing fertilizers and run-off. The NO_3^- values observed in the present study were low compared to results of some studies in Nigerian rivers (Igbinosa et al., 2012; Yusuf et al., 2017; Amah-Jerry et al., 2017; Anyanwu and Emeka, 2019). However, NO_3^- values recorded during this study were within or little below the results of Anyanwu and Ukaegbu (2019) and Kindele and Olutona (2014), both obtained in Nigeria.

Similarly, the spatial and temporal variations of NO_3^- in this study is in line with the spatial variation results in the study of Yusuf et al. (2017), who reported higher NO_3^- values between March and May in the Saba River, Osogbo, but they do not fall in line with the study of Makinde et al. (2015), who recorded higher NO_3^- values during dry season months (November to February) than during rainy season months (July to October) in the Ekerekana Creek and the Buguma Creek, River state, and Amah-Jerry et al. (2017), who obtained lower values of NO_3^- between March and May in the southeast of the Aba River, all in Nigeria. The spatial and temporal variations, especially the higher values obtained between March and May, could be attributed to early rains and fertilizers applied to early planted crop that empty NO_3^--containing materials into the river.

The SO_4^{2-} concentration values recorded in this study were rather low compared to related studies on the Nigerian rivers (Anyanwu, 2012; Makinde et al., 2015; Amah-Jerry et al., 2017). On the other hand, the present SO_4^{2-} values were within or slightly lower than the range of values obtained in some studies (Anyanwu and Emeka, 2019; Anyanwu and Ukaegbu, 2019). Similarly, the higher SO_4^{2-} values obtained in this study during the rainy season are comparable with Makinde et al. (2015), who reported higher values during the rainy season in the Ekerekana and Buguma Creeks, the Niger delta, and Amah-Jerry et al. (2017), who recorded higher values during the rainy season in the Aba River, southeast, both in Southeast Nigeria. The high values of SO_4^{2-} during the rainy season may be attributed to the oxidation of SO_3^{2-} to SO_4^{2-} from run-off loaded and decaying organic materials (Makinde et al., 2015).

Na^+ is always present in all-natural surface waters as a result of its salt solubility, and it is relatively abundant on earth. The values of Na^+ in most surface water are well below 5 mg/L (Anyanwu, 2012). The Na^+ values obtained in the present study were similar to the study of Anyanwu and Ukaegbu (2019) on the Ossah River, Umuahia, Southeast Nigeria. However, Na^+ values were low compared to Ikhuoriah and Oronsaye (2016) but slightly higher than Anyanwu and Emeka (2019) and Anyanwu et al. (2022).

K^+ is usually found in low values in natural waters due to relative resistance of rocks containing K^+ to weathering (Skowron et al., 2018). All aquatic organisms require K^+ for several metabolic processes, including growth and development. Furthermore, K^+ not only limits growth at low values but also can be toxic at sufficiently high values (Anyanwu and Ukaegbu, 2019). The values of K^+ recorded in this study were within the results range obtained by Anyanwu (2012). However, some recent studies on fresh waters (Matta et al., 2018; Anyanwu and Ukaegbu, 2019) reported quite lower K^+ values compared to the values recorded in this study.

Ca^{2+} is an essential component of many aquatic organisms, constituting part of plant cell walls, shells and bones (Chapman and Kimstach, 1996). Low Ca^{2+} values may cause osmotic problem and deformities in shell fish such as crayfish, oyster, crab, prawn, periwinkle, and aquatic snails (Hessen et al., 2017; Jeziorski and Smol, 2017). Ca^{2+} values recorded in this study were relatively lower compared to some studies (Ikhuoriah and Oronsaye, 2016; Anyanwu and Emeka, 2019; Anyanwu et al., 2022). However, the values were within the range recorded in the Ossah River, Umuahia, Abia state, Southeast Nigeria (Anyanwu and Ukaegbu, 2019). In this study, Ca^{2+} values were higher in rainy season months than in dry season months, and this could be probably a result of burnt shell via farmland

preparation that emptied into the river by wastewater. Higher Ca^{2+} values observed in the Akor River may be attributed to intensive farming activities by numerous farmers in communities along the river.

Mg^{2+} is available in many organic matters such as rock and forms an essential element for living organisms. Naturally, concentration of Mg^{2+} depends on the rock types along the watershed area, and its range in freshwaters is between 1 and > 100 mg/L. Very low ionic Mg^{2+} concentration in Ca^{2+}-deficient aquatic environment pose the greatest risk to aquatic organisms.

In this study, Mg^{2+} values recorded were low and within acceptable limits set by FMEnv (2011). Some recent studies carried out in Southeast Nigerian fresh waters also recorded low Mg^{2+} values. Anyanwu and Ukaegbu (2019) equally recorded values between 0.42 and 1.38 mg/L in the Ossah River, Umuahia. There is a seasonal variation with respect to Mg^{2+} values in the river; higher values were observed during the rainy season than in the dry season. This may be attributed to multiple factors such as physical weathering and farming activities coupled with early and heavy rains that could wash the weathered Mg^{2+}-contained materials into the Akor River.

The cation values obtained in this study were in the order of $Ca^{2+} > Mg^{2+} > Na^{+} > K^{+}$. The major cations order in this study agrees with the common trend observed in Nigerian inland fresh waters, in which Ca^{2+} and Mg^{2+} are the most important cations (Imevbore, 1970; Egborge, 1971; Anyanwu, 2012; Anyanwu and Ukaegbu, 2019). Despite the higher values of Ca^{2+} and Mg^{2+} recorded, the water of the river is soft.

4.2. Water quality indices

The results of water pollution status reflected the effects of seasons and anthropogenic activities. The seasonal variations may be associated with different human activities in different seasons of the year. Although, generally, the results indicate that the Akor River has a good water quality throughout the sampling periods. The results of quality indices of the Akor River were within the range obtained by Anyanwu and Umeham (2020), making it capable of sustaining biodiversity as well as crop irrigation.

5. Conclusions

Activities such as intensive farming, industrialization and waste discharge into surface water bodies have been a threat to the physical-chemical parameters of water bodies, and surface water bodies in Southeast Nigeria are not an exception. In this study, physical-chemical parameters were investigated. The study indicated that human (anthropogenic) activities, including sand mining, agricultural activities, washing of household utensils, swimming, etc. had not negative impact on the water quality according to the water quality indices. However, some parameters such as turbidity, pH, DO, BOD, and COD did not meet the standards. The pollution status of the Akor River depends on season and anthropogenic activities, but presently the river has a good status and is capable of sustaining biodiversity as well as crop irrigation.

Acknowledgements

The authors acknowledge John Ndukwe for his support during the water sampling and laboratory analysis.

Conflict of interests

The authors declare no conflict of interests.

References

Adeosun F.I., Adams T.F., Amrevuawho M.O. 2016. Effect of anthropogenic activities on the water quality parameters of federal university of agriculture Abeokuta reservoir. International Journal of Fisheries and Aquatic Studies 4(3): 104-108.

Al-Othman A.A. 2019. Evaluation of the suitability of surface water from Riyadh Mainstream Saudi Arabia for a variety of uses. Arabian Journal of Chemistry 12(8): 2104-2110. DOI: 10.1016/j.arabjc.2015.01.001

Amah-Jerry E.B., Anyanwu E.D., Avoaja D.A. 2017. Anthropogenic impacts on the water quality of Aba River, Southeast Nigeria. Ethiopian Journal of Environmental Studies and Management 10(3): 299-314. DOI: 10.4314/ejesm.v10i3.3

Anyanwu E.D. 2012. Physicochemical and some trace of metal analysis of Ogba River, Benin City, Nigeria. Jordan Journal of Biological Sciences 5(l): 47-54.

Anyanwu E.D., Emeka C.S. 2019. Application of water quality index in the drinking water quality assessment of a southeastern Nigeria river. Food and Environment Safety 18(4): 308-314.

Anyanwu E.D., Okorie M.C., Odo S.N. 2019. Macroinvertebrates as bioindicators of water quality of effluent-receiving Ossah River, Umuahia, Southeast Nigeria. ZANCO Journal of Pure and Applied Sciences 31(5): 9-17. DOI: 10.21271/ZJPAS.31.5.2

Anyanwu E.D., Ukaegbu A.B. 2019. Index approach to water quality assessment of a south eastern Nigerian river. International Journal of Fisheries and Aquatic Studies 7(1): 153-159.

Anyanwu E.D., Umeham S.N. 2020. Identification of waterbody status in Nigeria using predictive index assessment tools: a case study of Eme River, Umuahia, Nigeria. International Journal of Energy and Water Resources 4: 271-279. DOI: 10.1007/s42108-020-00066-5

Anyanwu E.D., Jonah U.E., Adetunji O.G. et al. 2022. An appraisal of the physicochemical parameters of Ikwu River, Umuahia, Abia State in South-eastern, Nigeria for multiple uses. International Journal of Energy and Water Resources 2022. DOI: 10.1007/s42108-021-00168-8

Bobor L.O., Umeh C.M. 2019. Physicochemical and microbiological water quality assessment of Aba Waterside River, Aba, Nigeria. Nigerian Journal of Environmental Sciences and Technology 3(1): 142-148.

Chapman D., Kimstach V. 1996. Selection of water quality variables. In: Chapman D. (Ed.), Water quality assessment: a guide to the use of biota, sediments and water in environmental monitoring (2nd Edition). Cambrige: University Press, pp. 74-132.

Danha C., Utete B., Soropa G., Rufasha S.B. 2014. Potential impact of wash bay effluent on the water quality of a subtropical river. Journal of Water Resource and Protection 6: 1045-1050. DOI: 10.4236/jwarp.2014.611099

Effendi H., Romanto B., Wardiatno Y. 2015. Water quality status of Ciambulawung River Banten Province based on pollution index and NSF-WQI. Procedia Environmental Sciences 24: 228-237. DOI: 10.1016/j.proenv.2015.03.030

Ewa E.E., Iwara A.I., Adeyemi J.A. et al. 2011. Impact of industrial activities on water quality of Omoku creek. Sacha Journal of Environmental Studies 1(2): 8-16.

Flura M.A., Alam A., Nima M.B. et al. 2016. Physicochemical and biological properties of water from the river Meghna, Bangladesh. International Journal of Fisheries and Aquatic Studies 4(2): 161-165.

FMEnv. 2011. National environmental (surface and groundwater quality control) regulations, s.i. no. 22, gazette no. 49, vol. 98. Abuja: Federal Ministry of Environment.

Goldschmidt T. 2016. Water mites (Acari, Hydrachnidia): powerful but widely neglected bioindicators – a review. Neotropical Biodiversity 2: 12-25.

Gupta S.K., Dixit S., Tiwari S. 2005. An assessment of heavy metals in surface waters of lower lake, Bhopal, India. Pollution Research 4: 805-808.

Harding L.W., Mallonee M.E., Perry E.S. et al. 2019. Long-term trends, current status, and transitions of water quality in Chesapeake Bay. Scientific Reports 9: 6709. DOI: 10.1038/s41598-019-43036-6

Hessen D.O., Andersen T., Tominaga K. et al. 2017. When soft waters becomes softer; drivers of critically low levels of Ca in Norwegian lakes. Limnology and Oceanography 62: 289-298. DOI: 10.1002/lno.10394

Igbinosa E.O., Uyi O.O., Odjadjare E.E. et al. 2012. Assessment of physicochemical qualities, heavy metal concentrations and bacterial pathogens in Shanomi Creek in the Niger Delta, Nigeria. African Journal of Environmental Science and Technology 6(11): 419-424.

Ikhuoriah S.O., Oronsaye C.G. 2016. Assessment of physicochemical characteristics and some heavy metals of Ossiomo River, Ologbo – a tributary of Benin River, Southern Nigeria. Journal of Applied Science and Environmental Management 20(2): 472-481. DOI: 10.4314/jasem.v20i2.30

Jeziorski A., Smol J.P. 2017. The ecological impacts of lakewater calcium decline on softwater boreal ecosystems. Environmental Reviews 25: 245-253. DOI: 10.1139/er-2016-0054

Joshua N.M., Nazrul M.I. 2015. Water pollution and its impact on the human health. Journal of Environment and Human 2.

Kindele E.O., Olutona G.O. 2014. Water physico-chemistry and zooplankton fauna of Aiba Reservoir Headwater Streams, Iwo, Nigeria. Journal of Ecosystems 11: 1-11. DOI: 10.1155/2014/105405

Makinde O.O., Edun O.M., Akinrotimi O.A. 2015. Comparative assessment of physical and chemical characteristics of water in Ekerekana and Buguma Creeks, Niger Delta Nigeria. Journal of Environment Protection and Sustainable Development 1(3): 126-133.

Matta G., Naik P.K., Machell J. et al. 2018. Comparative study on seasonal variation in hydrochemical parameters of Ganga River water using comprehensive pollution index (CPI) at Rishikesh (Uttarakhand) India. Desalination and Water Treatment 118: 87-95. DOI: 10.5004/DWT.2018.22487

Okereke I.J. 2014. An assessment of the physico-chemical parameters of Ihuku River. IOSR Journal of Environmental Science, Toxicology and Food Technology 8(1 Ver. I): 27-30.

Olalekan O.I., Oladipupo S.O., Habeeb A.Q. et al. 2012. Influence of human activities of the water quality of Ogun River in Nigeria. Civil and Environmental Research 2(9): 36-48.

Oluyemi E.A., Adekunle A.S., Adenuga A.A. et al. 2010. Physicochemical properties and heavy metal content of water sources in Ife North Local Government Area of Osun State, Nigeria. African Journal of Environmental Science and Technology 4(10): 691-697. DOI: 10.4314/ajest.v4i10.71334

Omer N.H. 2019. Water quality parameters. In: Summers K. (Ed.), Water quality: science, assessments and policy. London: IntechOpen, pp. 1-18. DOI: http://dx.doi.org/10.5772/intechopen.89657

Omole D.O., Longe E.O. 2008. An assessment of the impact of abattoir effluents on River Illo, Ota, Nigeria. Journal of Environmental Science and Technology 1(2): 56-64. DOI: 10.3923/jest.2008.56.64

Oribhabor B.J., Udoidiong O.M., Udoh D.F. et al. 2013. Evaluation of the ecological impact of human settlement on the water quality of lower Cross River, Nigeria. Journal of Ecosystems 2013(1). DOI: 10.1155/2013/840295

Osibanjo O., Adie G.U. 2007. Impact of effluent from Bodija abattoir on the physicochemical parameters of Oshunkaye stream in Ibadan City, Nigeria. African Journal of Biotechnology 6(15): 1806-1811. DOI: 10.4314/ajb.v6i15.57795

Parvez M.A., Uddin M.M., Kamrul I. et al. 2019. Physicochemical and biological monitoring of water quality of Halda River, Bangladesh. International Journal of Environmental and Science Education 14(4): 169-181.

Petlušová V., Petluš P., Zemko M. et al. 2019. Effect of landscape use on water quality of the Žitava River. Ekológia (Bratislava) 38(1): 11-24. DOI: 10.2478/eko-2019-0002

Skowron P., Skowrońska M., Bronowicka-Mielniczuk U. et al. 2018. Anthropogenic sources of potassium in surface water: the case study of the Bystrzyca river catchment, Poland. Agriculture, Ecosystems and Environment 265: 454-460. DOI: 10.1016/j.agee.2018.07.006

SON 2015. Nigerian standard for drinking water quality. Nigerian Industrial Standard (NIS 554-2015). Standards Organisation of Nigeria (SON), Abuja, Nigeria. p. 18.

Titilawo Y., Akintokun A., Shittu O. et al. 2019. Physicochemical properties and total coliform distribution of selected rivers in Osun State, Southwestern Nigeria. Polish Journal of Environmental Studies 28(6): 4417-4428. DOI: 10.15244/pjoes/81561

Ubwa S.T., Atoo G.H., Offem J.O. et al. 2013. An assessment of surface water pollution status around Gboko abattoir. African Journal of Pure and Applied Chemistry 7(3): 131-138. DOI: 10.5897/AJPAC2013.0486

USEPA. 2022. CADDIS Volume 2 – pH. Low pH - Checklist of sources, site evidence and biological effects. U.S. Environmental Protection Agency, Washington DC. URL: https://www.epa.gov/caddis-vol2/ph (last access March 30, 2022)

Wang J., Liu X.D., Lu J. 2012. Urban river pollution control and remediation. Procedia Environmental Science 13: 1856-1862.

Yusuf O.A., Adewole H.A., Olaleye V.F. 2017. Assessment of the water quality of Saba River, Osogbo, Nigeria. Notulae Scientia Biologicae 9(2): 188-195. DOI: 10.15835/nsb9210001

Zhang X., Wu Y., Gu B. 2015. Urban rivers as hotspots of regional nitrogen pollution. Environmental Pollution 205: 139-144.

Limnology and Freshwater Biology 2022 (2): 1229-1243 DOI:10.31951/2658-3518-2022-A-2-1229

Original Article

ISSN 2658-3518
LIMNOLOGY FRESHWATER BIOLOGY
www.limnolfwbiol.com

Cytomorphology of the 'wound healing' process in the green filamentous algae, *Ulothrix zonata* (F. Weber & Mohr) Kützing 1833

Natyaganova A.V.*, Mincheva E.V., Bukin Yu.S.

Limnological Institute, Siberian Branch of the Russian Academy of Sciences, Ulan-Batorskaya Str., 3, Irkutsk, 664033, Russia

ABSTRACT. For the first time, we present a cytomorphological description of the self-healing (repair) process of damaged thalli sites, 'wound healing', in the green filamentous algae, *Ulothrix zonata* (F. Weber & Mohr) Kützing 1833. In the filaments of this species from Lake Baikal and the Angara (Baikal outflow), Zhilishche (Baikal inflow) and Ida (Angara inflow) rivers, light microscopy methods revealed dome-like and conical protrusions and elongations of transverse cell walls directed into adjacent dead (without protoplast) and defective (with deformed chloroplasts) cells. At the same time, there were mostly patterns where two cells formed protrusions directed into the same damaged filament site between them, i.e. towards each other. The growth of previously unconnected cells towards each other led to their convergence and adjacency. This had two important physiological consequences that ensured the restoration of the filament integrity. The first consequence was the formation of intercellular junctions. The second one was the fusion of the protoplasts and nuclei of the adjacent cells (cell fusion) with the formation of vegetative polyploid cells with increased size. During subsequent divisions of these cells, extended areas emerged with a two- to three-fold increase in the diameter of the algal filaments. It was also found that the process of 'wound healing' promoted the development of giant hypnospores. We showed that the H-shaped septa between cells of filamentous algae were not thickenings of the outer walls but the sheaths of the dead cells preserved after this reparation process. Analysis of the 'wound healing' patterns revealed that the *Ulothrix* cell nuclei did not migrate to the polarized regions of the cells but retained their central position, which testifies to their fixation in the protoplast. We observed sporadic cases of the development of lateral filaments in *U. zonata* were due to the self-repair of defective cells and their subsequent division during 'wound healing'. A comparison of various cell deformations allowed us to determine the characteristic stages of the 'wound healing' process in *U. zonata*, which have some similarities and differences with those in marine red filamentous algae. Our study indicates that 'wound healing' is an evolutionarily developed and genetically programmed adaptation that may be widespread in the population of filamentous algae.

Keywords: filamentous algae, *Ulothrix zonata*, wound healing, repair, cell fusion

1. Introduction

The integrity of algal thalli is constantly exposed to various environmental factors: abiotic and biotic. They include water currents and wave action, abrasion from sand and other fine-grained soils, grazing of fish and benthic animals (molluscs, crustaceans, etc.) as well as attacks by pathogenic fungi, bacteria and protozoa (Gachon et al., 2010). Moreover, programmed cell death may also be a mechanism of thalli damage, especially for filamentous algae (Dingman and Lawrence, 2012; Garbary et al., 2012). If damage is not quickly repaired, the body can fall apart at the sites of damaged or dead cells. Therefore, repair is an important life process for representatives of aquatic flora. Information about the ability of macroalgae to repair the regions of thalli with dead or damaged cells began to appear in the scientific literature as early as in the 19th century (Janczewski, 1876 cited by Lewis, 1909). Interestingly, the term 'regeneration' was originally used to describe such cases. However, already in subsequent publications concerning the study of repair in algae, there were expressions most likely appropriate for representatives of animal world: 'methods of healing' and 'wound healing' (Nichols, 1922; Höfler, 1934). According to the literature, to date, these expressions have also become generally accepted for the description of repair processes in macroalgae (Waaland and Cleland, 1974;

*Corresponding author.
E-mail address: avn61@mail.ru

Received: January 11, 2022; ***Accepted:*** May 20, 2022;
Available online: June 21, 2022

La Claire, 1982; Kim et al., 1988; Menzel, 1988; Kim and Fritz, 1993; Mine et al., 2008; Hoermayer and Friml, 2019).

The process of 'wound healing' in the modern sense and in the application to the animal body is a complex of reactions and interactions of cells and 'mediators' that ensure the replacement of damaged cells or tissues with new healthy ones (Wang et al., 2018; Wilkinson and Hardman, 2020). Unlike animal cells, plant cells are enclosed in rigid walls and cannot migrate to the damaged site. Therefore, their protective mechanisms, namely regeneration and repair, are based on three cytological strategies: oriented cell division, acquisition of new cell fates and directional cell elongation (polarized growth or tropism) (Hoermayer and Friml, 2019; Mironova and Xu, 2019). Oriented cell division is the involvement in mitosis of any cell adjacent to the damaged site, even of differentiated cells, i.e. those that have previously left the cell cycle (Hoermayer and Friml, 2019). Acquisition of new cell fate means either dedifferentiation or transdifferentiation of cells surrounding the damaged site. Dedifferentiation refers to any cellular change towards a less specialized, more juvenile and more pluricompetent state (Sugiyama, 2015; Mironova and Xu, 2019), while transdifferentiation is defined as a switch from one specialized cell type to another (Nguyen and McCurdy, 2016; Mironova and Xu, 2019). Directional (polarized) cell growth (or tropism) occurs thanks to irreversible elongation, a very rapid growth type that is only characteristic of plant cells (Polevoy, 1998; Baluska et al., 2003; Cole and Fowler, 2006; Girloy, 2008; Obroucheva, 2008; Cells, 2007; Jaffar and Davidson, 2013). This process is based on three coordinated stages: i) swelling of the central vacuole resulted from the influx of water; ii) loosening of the cell wall allowing its expansion and iii) formation of the cell swelling force vector in a certain direction, i.e. cell polarization. It is also generally accepted that growth by elongation is one of the ways, in which plants move. It first appeared in filamentous algae, enabling the attached plants to move to food sources and other resources (Esmon et al., 2005).

In the vast majority of studies on the 'wound healing' process in algae, representatives of the marine flora with a siphonal and siphonocladal arrangement of thalli, as well as with giant coenocyte (multinucleate) cells reaching millimeter and even centimeter sizes, served as study objects (for reviews, see Menzel, 1988; Mine et al., 2008). Mechanisms of 'wound healing' in macroalgae from freshwater bodies were studied only in a few species that also had giant coenocytic cells (Nichols, 1922; Foissner, 1988; Foissner and Wasteneys, 1997). To date, it has been shown that, unlike higher plants, individual damaged cells can be restored in algae. For instance, the process of 'wound healing' in cells of siphon algae includes the rapid repair of cytoplasmic damage, the preliminary sealing of wounds in cell wall with plugs consisting of polysaccharides or peptides, or their mixture and then the final regeneration of a new cell wall over the restored surface (Burr and West, 1972; Colombo and De Carli, 1980; Menzel, 1988; Mine et al., 2008). The restored cells continue to function normally. Most siphonocladal algae respond to mechanical trauma by contraction of the protoplast or by the formation of numerous cytoplasmic aggregates, from which regeneration of new thalli can subsequently occur (Tatewaki and Nagata, 1970; La Claire, 1982; Kim et al., 2001). In marine red algae with branching filamentous thalli, damaged intercalary cells are not repaired but replaced by new ones (Lewis, 1909; Waaland and Cleland, 1974; Kim et al., 1988). At the same time, two types of specialized somatic cells are formed: from one to several upper rhizoid cells and lower shoot cells. They grow from the transverse walls of adjacent cells towards each other into the damaged cells and either fusion to form a single cell or a pit connection. Thus, these new cells ultimately replace the dead cell, completing the wound healing response and restoring the continuity of the filament. Also, it was shown that adjacent cells themselves can continue to grow into the lumen of damaged cells and form pit connections upon meeting, thereby repairing the filament (Kim et al., 1988). Notably, all published results were obtained empirically, i.e. this process was studied in the thalli of macroalgae with intentionally damaged or killed cells. Such an experimental and rather intensive study of 'wound healing' process in algae not only allowed the description of its pattern but also elucidated the role of cell organelles as well as provided identification and isolation of the substances involved in this process (Burr and West, 1972; Waaland and Watson, 1980; Watson and Waaland, 1986; Menzel, 1988).

Despite many years of intensive studies of 'wound healing' process in macroalgae, the information about this phenomenon in freshwater inhabitants is very limited. There is also a lack of scientific information about how 'wound healing' occurs in algae under natural conditions. In this study, we demonstrate that this process can be observed and studied not only in artificially damaged cells but also in naturally damaged ones in samples of macroalgae taken from their habitat.

2. Materials and methods

U. zonata (girdle-shaped Ulothrix) is a member of rather large genus from the order of Ulothrix algae (Ulotrichales). It is widespread in the coastal zone of clean and well-aerated fresh and brackish water bodies, forming dark and yellow-green fouling on various objects submerged in water: stones, wood residues, hydraulic structures, ship bottoms, etc. (Fig. 1A, 1B). This typical representative of macrophytobenthos is considered one of the most studied species of the genus with a clearly established development cycle (Shyam and Saxena, 1980). The history of the study of *U. zonata* dates back to 1804, the year of its first description when this species was named *Conferva zonata*, and in 1833 it was first classified as *Ulothrix zonata* (Weber and Mohr, 1804; Kützing, 1833; Lokhorst and Vroman, 1972). Foreign and Russian algologists indicated a high degree of polymorphism of this species both in nature and in cultivation, which resulted in the description of many

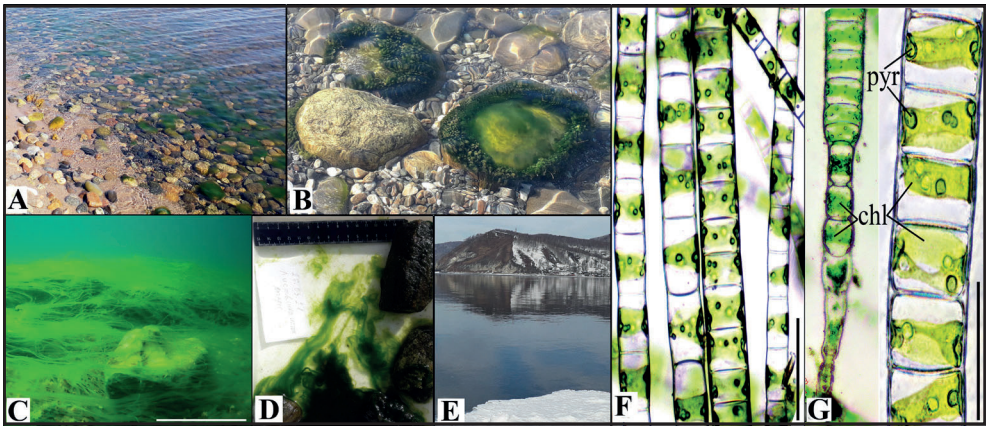

Fig.1. General information about the green filamentous algae, *Ulothrix zonata* (F. Web. & Mohr.) Kützing 1833 (girdle-shaped Ulothrix). One of the coastal areas of Lake Baikal with stones overgrown with Ulothrix in summer (A, B); *U. zonata* bloom with filament strands reaching a meter depth at a depth of 5 m (C, D) in the Angara River source in late March 2021 (E); live filaments of *U. zonata* under a light microscope (F, G); basal (left) and intercalary (right) fragments of a live filament with typical vegetative cells (G). Designations: chl – chloroplasts and pyr – pyrenoids. Scale bars: 0,5 m (C); 50 μm (F, G).

of its varieties (Lokhorst and Vroman, 1972; Shyam and Saxena, 1980; Moshkova and Gollerbakh, 1986; Izhboldina, 2007). In Lake Baikal, *U. zonata* begins to develop in April in the coastal zone on the lower surfaces of ice hummocks (Bondarenko et al., 2009). After the release of the water column from the ice, its large-scale vegetation begins along the entire coast at depths from 0 to 1.5 m, with subsequent formation of an entire vegetation belt (Meyer, 1930). At the same time, in the past decade, abundant Ulothrix blooms have begun in March at depths of 0.5 to 3–5 m near the source of the Angara River free of the ice (Fig. 1C–1E). Despite the still snowy and icy shore, *U. zonata* successfully vegetates here, and strands of its filaments reach a meter length at depths of 3 to 5 m. This is associated with an intense anthropogenic impact on the aquatic environment in the Listvyanka settlement (Kravtsova et al., 2014). Taxonomic analysis revealed only two varieties of this algae in Lake Baikal: *U. zonata* and *U. zonata* var. *zonata* (Izhboldina, 2007).

U. zonata thalli samples were collected from stones during the expedition in June 2020 at Lake Baikal in the coastal splash zone at depths of 0 to 1 m near the following sampling stations: Polovinny Cape (51°47'52.8"N 104°21'04.8"E), Kultuk (51°43'39.9"N 103°43'21.3"E) and Marituy (51°47'13.5"N 104°13'16.2"E) settlements, and the Katorzhanka River (51°47'59.7"N 104°37'40.6"E). In August 2020, samples were taken from stones near the shore from the Angara River basin: (52°14'23.4"N 104°19'27.6"E), (52°15'00.5"N 104°17'05.7"E). Thereafter, in March 2021, Ulothrix thalli were sampled in the Angara River source in the vicinity of the Listvyanka settlement from stones near the shore and from a depth of 5 m (51°50'51.5"N 104°52'17.4"E). Additionally, we studied summer samples of *U. zonata* from the Zhilishche River (July 2021) (51°54'00.7 "N 105°03'51.4 "E) flowing into Lake Baikal and the samples from the Ida River, the Angara's tributary (53°09'54.6"N 104°12'43.1"E), which were collected in July 2017. For light microscopy, temporary cytological preparations were made from live and vitally (in vivo) unfixed filaments stained with acetoorcein (La Cour, 1941; Pausheva, 1988). For vital staining, live samples were immediately placed and stored in Eppendorf tubes with dye. Temporary cytological preparations were also prepared from Ulothrix thalli fixed in a mixture of ethyl alcohol and acetic acid (3:1) and stained with hematoxylin (Wittmann, 1965; Pausheva, 1988). Live filaments were distributed using tweezers or needles under a stereomicroscope on a glass slide in a drop of water, covered with a cover slip and examined under an Olympus CX23 LED microscope with a ToupCam 9.0 MP series digital camera. Thalli samples stained with acetoorcein and hematoxylin were rinsed in 45% acetic acid, dried on filter paper and distributed in a drop of lactic acid (80%) on a glass slide under a stereomicroscope (La Cour, 1941; Wittmann, 1965; Pausheva, 1988). Then they were covered with a cover slip and were also examined under a microscope coupled with photodocumentation. The species identification of the specimens was carried out according to N.A. Moshkova and M.M. Gollerbakh (1986) and L.A. Izhboldina (2007).

3. Results and discussion

Based on morphological characteristics, all algae samples collected were determined as the species *U. zonata* (girdle-shaped Ulothrix). According to the taxonomic description (Lokhorst and Vroman, 1972; Moshkova and Gollerbakh, 1986; Izhboldina, 2007), these algae have the shape of long (from 5 cm to 5 dm), strait or variously curved green or yellow-green (unbranched) filaments consisting of one series of cells tightly attached to each other (Fig. 1F, 1G). Typical vegetative cells of this species are characterised by cylindrical or barrel shape and chloroplasts in the form of median ring (girdle) with several large pyrenoids (Fig. 1G). During the transition of cells to reproductive functions (sporogenesis, gametogenesis or formation of hypnospores), their shape does not change, i.e. sporangia, gametangia and cells with hypnospores have the same cylindric shape (Lokhorst and Vroman, 1972). Cell width determines the width of filamentous Ulothrix thalli, varying from 11 to 83 μm. The length of

cells varies depending on the width of the cells (Fig. 1F, 1G): it can be six times longer, equal to or three times shorter than the width, while usually in the juvenile filaments of the species of the genus *Ulothrix*, the length of cells significantly exceeds the width, i.e. they look narrow and long (Moshkova and Gollerbakh, 1986; Izhboldina, 2007). Throughout their length, filaments often consist of cells with the same width (Fig. 1F, 1G), but there are also thalli with sites containing a series of cells having a shorter or longer width than the entire filament (Fig. 1G, basal fragment).

In all studied samples of *U. zonata* filaments, we revealed various deviations from the typical cilindrical shape in vegetative and reproductive cells with zoo- and hypnospores, which indicated the 'wound healing' process previously described in marine red filamentous algae (Lewis, 1909; Waaland and Cleland, 1974; Kim et al., 1988; Kim and Fritz, 1993).

3.1. Directional (polarized) cell growth in filaments, a characteristic sign of the onset of the 'wound healing' process in the *U. zonata* green algae

Directional (polarized) growth of typical vegetative cells is a characteristic morphological sign of the onset of the 'wound healing' process in the filaments of *U. zonata*, as evidenced by dome-shaped (Fig. 2A–2G) and conical (Fig. 2F, 2H) protrusions and elongations of their transverse walls. At the same time, frequent episodes of protrusions of both transverse walls of one cell indicate that polarized growth can occur in two directions and change her shape to spherical (Fig. 2D). It should be noted that such protrusions of cell wall always closely adjacent to dead cells (without protoplast) and defective cells (Fig. 2A–2H, marked with asterisks) and, moreover, are always directed inside their space. Anatomically altered cells with chloroplasts that were deformed or changed colour due to physiological or mechanical damage are called here as defective. The number of dead or defective cells can be one-two (Fig. 2A, 2B, 2D, 2E, 2G, 2H) or more (Fig. 2C, 2F,), i.e. they can occupy rather long sites in the filaments and are always clearly visible between dome-shaped and conical protrusions and elongations of cell walls. Also, sporangia (the reproductive cells) carry out directional growth into adjacent cells released from zoospores (Fig. 2E). Notably, protrusions of the walls only in one cell adjacent to defective filament sites are rather rare. As a rule, such deformations of transverse walls occur in both cells, between which one or several defective or dead adjacent cells appear. For example, Figure 2F shows a fragment of a filament, in which one of the vegetative cells (on the left) formed a clearly visible dome-shaped protrusion of the transverse wall directional to a series of several defective cells. On the opposite side of this series (on the right), another vegetative cell transformed into a rather extended cone that was also directional to the same series. Thus, these cells grow directionally towards each other.

Noteworthy is that polarized growth in *U. zonata* does not prevent mitosis and does not change the

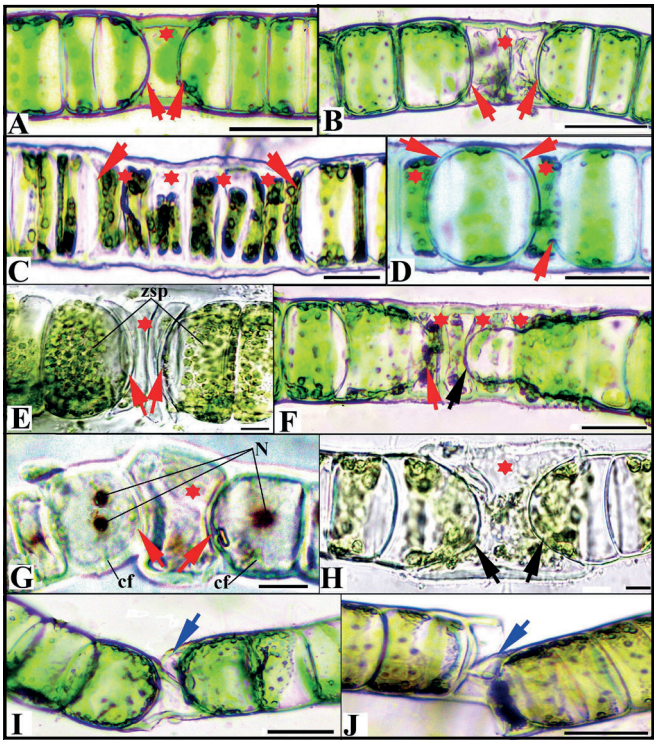

Fig.2. Typical signs of the onset of the 'wound healing' process and its interruption in filaments of the *U. zonata* green algae. Protrusions and elongations of the cell walls are marked with arrows: red – dome-shaped (A–G) and black – conical (F, H). The blue arrows indicate cases of interruption of the 'wound healing' process: deformation (I) and rupture (J) of filaments at vulnerable sites with dead cells. Asterisks mark defective (anatomically altered cells with chloroplasts that were deformed or changed colour due to physiological or mechanical damages) and dead (without protoplast) cells. (E) – filament fragment with sporangia containing zoospores. Designations: zsp – zoospores; cf – cleavage furrow and N – cell nuclei. Photomicrographs of live filament specimens (A–F and H–J) and photomicrograph of a filament specimen fixed in ethyl alcohol and acetic acid (3:1) and stained with hematoxylin (G). Scale bars: 50 μm (A–D, F, I, J) and 10 μm (E, G, H).

behaviour of the nuclei in the growing cells. Nuclei retain their location in the centre of the cell and their role in cell division. For instance, Figure 2G shows that a cleavage furrow (cf) and two juvenile nuclei (N) occurred in the centre of one of the cells (on the left). In another cell (on the right), cleavage furrow (cf) began to form, and already two sets of genetic material were visible in the nucleus (N). In other words, these cells performed division and directional growth simultaneously. At the same time, patterns of deformation and rupture of filaments at the most vulnerable sites with defective or dead cells testify to the possible interruption of the 'wound healing' process and another likely outcome such as filament rupture (Fig. 2I, 2J). The size and fate of the fragments can be different because they both would become independent plants. Attached thallus fragment would continue its activity. The free fragment of the filament would be carried away from the original filament, and, only after attaching to the substrate, it would be able to grow further. In this case, it would serve to spread the species

because thalli fragmentation is one of the methods of vegetative propagation in all algal divisions, especially in filamentous algae (South and Whittick, 1990).

3.2. Convergence and adjacency of previously unconnected cells during 'wound healing' in filaments of *U. zonata*

Analysis of images of directional cell growth, namely dome-shaped and conical protrusions of their transverse walls, revealed that such modifications are dynamic. Progressive lengthening of the cell wall bulges led to convergence (Fig. 3A–3C) and adjacency of previously unconnected vegetative cells (Fig. 3D–3J). By the moment of adjacency, transverse cells could either retain the correct form or deform. In the first case, both cells developed equally convex transverse walls that were evenly adjacent to each other in the centre of a dead or defective cell (Fig. 3D, 3E). In the second case, cells formed different curvatures in walls free of interconnection so that their attachment to each other looked uneven (Fig. 3F–3H) and even as avoidance of contact (Fig. 3I, 3J). Obviously, with uneven attachment during directional growth, such cells experienced resistance from defective cells, in which vital processes were still preserved. This could cause curvature of cell walls and change in the direction of cell growth. The presented images also indicate that during the convergence and attachment of cells to each other, their nuclei retained their central position and continued to perform their functions in the cell cycle (Fig. 3C, 3J). For example, Fig. 3C shows that the nucleus occupies the central area of the cell with a pronounced conical elongation (on the right), and doubled genetic material is also visible in it, indicating nuclear division. There is also an emerging cell cleavage furrow (cf).

Notably, intercellular convergence and adjacency during 'wound healing' occurred within defective and dead cells that were still visible (Fig. 3A–3J, red asterisks). In other words, directional growth, convergence and adjacency of previously unconnected cells took place in a space protected by cell walls. This suggests that intercellular recognition and adhesion occured under these conditions, which was an important result at this stage (Jarvis et al., 2003).

3.3. Completion of the 'wound healing' process in filaments of *U. zonata*

Comparison of shapes of vegetative cells and configurations of their intercellular walls in filaments of the studied *U. zonata* specimens revealed that completion of the 'wound healing' process (i.e. the restoration of the filament integrity) in this green algae occurred according to the following different cytological scenarios: i) formation of junctions between cells directionally growing into the same defective section of the filament, which were not previously interconnected; ii) fusion of cells directionally growing into the same defective area of the filament, which were not previously interconnected; iii) restoration of viability and preservation of individuality of the

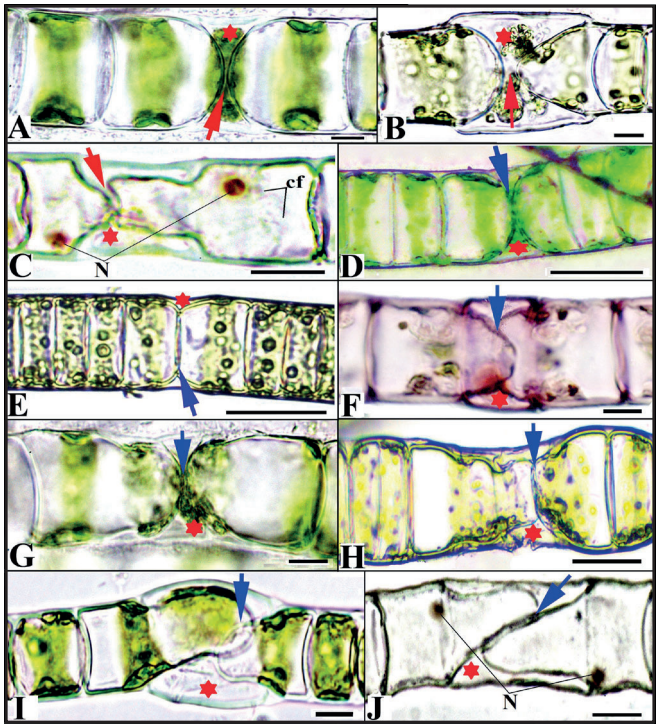

Fig.3. Cell convergence and adjacency during the 'wound healing' process in *U. zonata* filaments. Convergence of transverse walls of vegetative cells inside defective and dead adjacent cells through dome-shaped and conical protrusions and elongations (A–C). Attachment of previously unconnected vegetative cells to each other (D–J). The red arrows indicate narrow spaces between cells growing towards each other; blue arrows indicate areas of mutual cell contacts. Asterisks mark defective (anatomically altered cells with chloroplasts that were deformed or changed colour due to physiological or mechanical damages) and dead (without protoplast) cells. Designations: N – cell nuclei and cf – cleavage furrow. Photomicrographs of live specimens (A, B, D, E, and G–I); photomicrograph of a specimen with in vivo staining with acetoorcein (F); photomicrographs of specimens fixed in ethyl alcohol and acetic acid (3:1) and stained with hematoxylin (C and J). Scale bars: 10 μm (A, B, F, G, I, and J) and 50 μm (C–E and H).

defective cells during the directional growth of adjacent cells into their space. The first two scenarios led to the same result: the complete replacement of defective and dead cells by adjacent cells. The third scenario is an occasional event that leads to the development of a lateral filament from repaired defective cells.

3.3.1 Formation of junctions in previously unconnected cells

Based on the curved intercellular septa, trapezoid and some other non-cylindrcal shapes of vegetative cells in the *U. zonata* filaments among the studied samples, the convergence and adjacency of previously unconnected cells during directed growth to each other might result in the formation of an intercellular junction (Fig. 4). At the same time, in the case of even adjacencies of the adjoining cell walls, typical cellular septa were formed (Fig. 4A, 4B). They looked parallel to other transverse septa in filaments, and the connected cells themselves might not be deformed

and be almost indistinguishable from the adjacent ones. With uneven wall adjacencies, the conncted cells did not have a typical cylindrical shape and parallel intercellular septa (Fig. 4C–4G). In some cases, parallel septa of reduced diameter were formed between cells in the form of closed truncated cones (Fig. 4C). Moreover, sometimes there were connected cells of a very bizarre shape with significantly curved intercellular septa (Fig. 4E–4G). Such patterns arose in filaments apparently due to incompletely suppressed vital processes in defective cells, in which adjacent cells carried out directional growth. In these cases, there also might be the competition of cells for vital resources, which takes place in the recovery processes (Kravez, 2008). Light microscopy analysis of the samples revealed that the sheaths of dead cells could sometimes be preserved (Fig. 4H) and subjected to bilateral compression of adjacent cells growing within them. They could remain between cells in compressed form and contribute to thickening of the intercellular septa. Light microscopy did not allow us to identify and determine the type of emerging intercellular junctions. Nevertheless, it is acknowledged that a common type of intercellular junction in Ulothrix algae is plasmodesmata similar to those in higher plants (Floyd et al., 1971; Ehlers and Kollmann, 2001; Cells, 2007). They are thin tubular cytoplasmic channels that pass through the cell wall and connect two adjacent cells. The number and structure of plasmadesmata can vary depending on the cell and change in individual cells. This type of intercellular junction is a functional analogue of gap junctions in animals (Cells, 2007). Primary plasmadesmata are formed during cell division at the cytokinesis stage. In cells that are not products of a single division, there is also a mechanism for the formation of secondary plasmadesmata by partial destruction of the cell wall (Ehlers and Kollmann, 2001).

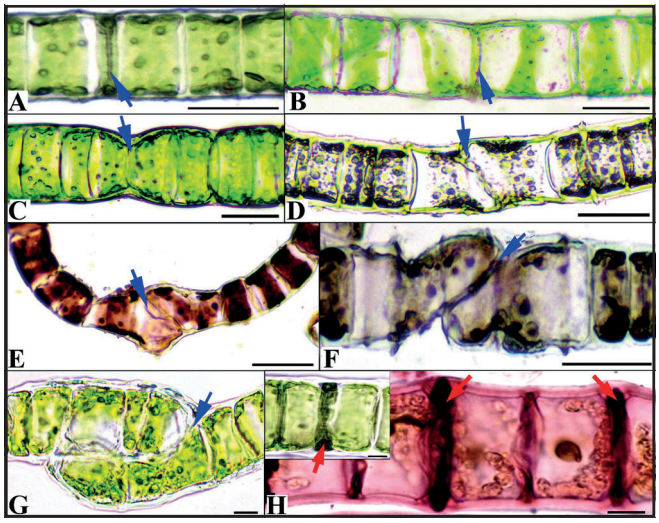

Fig.4. Completion of the 'wound healing' process in *U. zonata* filaments by formation of intercellular junctions. The blue arrows indicate intercellular septa formed with regular and even adjacencies (A, B) and irregular and uneven adjacencies of the adjoining walls (C–G). In the first case, intercellular walls are not deformed and are parallel to others; the shape of the cells almost does not differ from the typical one. In the second case, the formed intercellular septa have reduced diameter (C) or are deformed and not parallel to other septa (D–G), while the shape of the cells is significantly altered. The red arrows (H) mark the thickening of the intercellular septa due to compressed sheaths of dead cells (the insert shows live cells between which there is a compressed sheath of a dead cell). Photomicrographs of live specimens (A–D, G, and H (insert)) and photomicrographs of specimens stained in vivo with acetoorcein (E, F and H). Scale bars: 50 μm (A–F) and 10 μm (G, H).

3.3.2. Cell fusion and formation of giant vegetative cells

In addition to the cells of atypical noncylindrical shape in the studied samples, there were vegetative cells that were two to four times larger than the size of typical cells. These giants are evidence of cell fusion during 'wound healing' in *U. zonata*. Perhaps, in some cases of adjacent cells in the state of growth by elongation and with loosened cell walls, conditions arise, which promote the restructuring and fusion of their sheaths followed by the fusion of their protoplasts and nuclei. The fusion mechanism of plant vegetative cells with solid cell walls has not yet been fully elucidated. The possible expansion of intercellular channels (plasmodesmata) in the zones of contact cells and the effect of viruses or animal larvae on the dissolution of the solid cell wall were hypothesized (Maruyama et al., 2016). Thus, during directional cellular growth towards each other, interacting cells not only form intercellular junction, but also fuse into one giant vegetative cell, thereby 'healing the wounds' by restoring morphological integrity of the filament (Fig. 5A, 5B). During subsequent divisions, this cell gives rise to the same generation, leading to the appearance of extended sites with a sharp two- to four-fold increase in the filament diameter (Fig. 5C, 5D). This is reflected in one of the species traits of *U. zonata*: "…filamets of the same thickness throughout the length or randomly thickening or thinning…" (Moshkova and Gollerbakh, 1986). The cell fusion process is probably especially relevant for the onset of algal filament growth, which begins with a rather narrow basal cell with a lower level of ploidy than in other cells (Fig. 2C, basal filament fragment on the left). Furthermore, the localization and size of cell nuclei in such giant cells in cytological preparations from the *U. zonata* filaments fixed in ethyl alcohol and acetic acid fixative and stained with hematoxylin indicated karyogamy (cell fusion). In these giant cells, patterns of convergence (Fig. 5E, 5F) and fusion (Fig. 5G) of two nuclei from former typical cells, as well as patterns of significant differences of their nuclei from the nuclei of adjacent cells, were clearly visible. For example, Fig. 5H shows that the nucleus (1) of the giant cell is two to four times greater than the size of adjacent dividing (2) and juvenile nuclei (3), respectively. Obviously, the nuclei of giant cells contain an increased amount of genetic material, i.e. they are polyploid. Notably, the proximity of two nuclei is typical with the completion of division of typical vegetative cells, but in these cases, cell cleavage furrows can always be visible between the two nuclei (Fig. 2G; 5H – cf), which was not detected

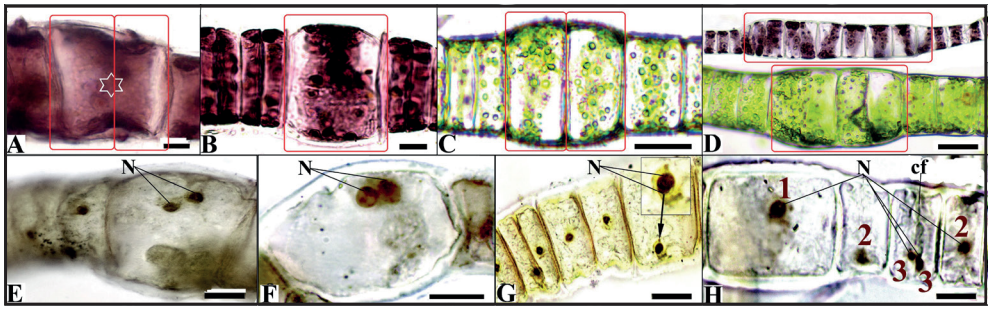

Fig.5. Completion of the 'wound healing' process in the *U. zonata* filaments by cell fusion and the formation of giant (polyploid) vegetative cells. The red rectangular contours indicate two vegetative cells in the fusion phase (A) (an asterisk marks the area of dissolved intercellular walls); the giant vegetative cell resulted from the fusion of two typical cells (B); two giant vegetative cells formed after division of one giant cell (C); thickened sections of the filaments formed by the division of giant vegetative cells (D); convergence of nuclei in giant cells (E, F); karyogamy (fusion of nuclei) in the giant cell (G) (the insert shows enlarged area indicated by the arrow); nuclei marked with the following numbers (H): (1) in the giant cell; (2) in dividing cells and (3) in juvenile typical vegetative cells. It is obvious that the nucleus of the giant cell (1) is two times larger than the nuclei of dividing cells (2) and four times larger than the nuclei of juvenile cells (3). Designations: N – cell nuclei and cf – cleavage furrow. Photomicrographs of specimens with in vivo staining with acetoorcein (A, B and D (upper filament fragment)), photomicrographs of live specimens (C, D (lower filament fragment)) and photomicrographs of specimens fixed in ethyl alcohol and acetic acid fixative (3:1) and stained with hematoxylin (E–H). Scale bars: 10 μ (A, B and E–H) and 50 μ (C, D).

during the convergence of nuclei in giant cells. Owing to their sizes (up to 100 μm in length and width) that are two to four times larger than the width or/and the length of typical filament cells, such vegetative cells were clearly distinguished in filaments even at the smallest magnification of a light microscope (x40).

3.3.3. Restoration of viability in defective cells during 'wound healing'

Microscopy of *U. zonata* filament samples indicated that sometimes defective cells themselves resotored their viability during "wound healing" (Fig. 6). Under the influence of directional growth of adjacent cells, they underwent significant deformation (Fig. 6A–6C). The presented figures indicate self-restoration of defective cells even in a significantly deformed cellular shape (Fig. 6B, 6C). The increased turgor pressure exerted on them by polarized growth of adjacent cells may also change the orientation of the preprophase bands of microtubules and actine filaments of the cortex, i.e. cytoplasmic structures that determine the direction of the cell division plane in vegetative cells (Brown and Lemmon, 2001; Cells, 2007). This is evidenced by sporadically occurring patterns of lateral filament development from deformed cells, the division of which was directed perpendicular to the main filament (Fig. 6B, 6D). Nevertheless, the images presented show that the directional growth of adjacent cells ends according to one of the above scenarios: the formation of intercellular junctions and typical transverse septa (Fig. 6C, 6D). Perhaps, there also may be cell fusion.

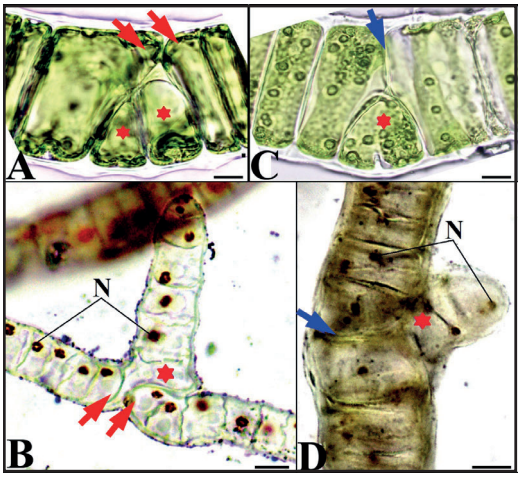

Fig.6. Restoration of viability in defective cells during the 'wound healing' process in *U. zonata*. Defective cells are marked with red asterisks. The red arrows indicate cells with directional growth (A, B) into adjacent defective cells. The blue arrows indicate transverse intercellular septa (C, D) formed during the directional growth of cells into defective cells. Sites of the thalli with the onset of the growth of new filaments from the defective cells, the mitotic division of which occurs in a plane perpendicular to the direction of the filament (B, D). Designations: N – cell nuclei. Photomicrographs of live specimens (A, C) and specimens fixed in ethyl alcohol and acetic acid (3:1) and stained with hematoxylin (B, D). Scale bars: 10 μm.

3.4. 'Wound healing' promotes the development of giant hypnospores in *U. zonata*

In addition to giant vegetative cells, there were huge cells with gigantic hypnospores (up to 100 μm in diameter) in the *U. zonata* specimens. Hypnospores are structures for asexual reproduction (Starmach, 1972; Bullock, 1978; Vasser et al., 1989). According to available descriptions, from 1 to 4 large and up to 32 small hypnospores can develop in the normally vegetating cell of *U. zonata*, which completely fill its volume. In other words, a single hypospore can grow to the size of a typical filament cell. Their characteristic features are a thick dense sheath and the lack of flagella, and during the development, the cytoplasm of the parent cell is not used entirely, and its sheath does

not participate in the formation of their integuments. Hypnospores can remain inside the parent cell for a long time and germinate into numerous filaments there. Our analysis revealed that sometimes typical vegetative cells carried out directional growth into cells with developing hypnospores (Fig. 7A). Perhaps, the transition of cells to this form of reproductive function significantly changes their typical vegetative state, which is a stimulus for adjacent cells to directed growth. Their growth into the same cell with developing hypnospore may also result in the fusion of all the three into one vast cell section (Fig. 7B, 7C). Thus, the conditions for the further development of the hypnospore are created, leading to the formation of its enormous size, 4–6 times the size of typical cells (Fig. 7D, 7E). The patterns that we identified also indicated that developing hypnospore can be displaced by two vegetative cells beyond the algal filament but remain connected to it and continue its growth in the already free space, where it can also reach gigantic sizes (Fig. 7F–7I). Hypnospore-displacing vegetative cells can fusion to form an enlarged polypoid vegetative cell (Fig. 7H) or build an intercellular junction (Fig. 7I). The presented photos clearly show the honeycomb structure of hypnospores, testifying to the development of numerous microspores in them, each of which can give rise to an individual algal filament (Bullock, 1978). Therefore, the 'wound healing' process in the *U. zonata* filamentous algae not only leads to the restoration of the filament integrity but also contributes to the reproductive function of the species.

3.5. Scheme of the 'wound healing' process in *U. zonata* and comparison of the results with data from the literature

The above patterns of the 'wound healing' process in green filamentous algae, *U. zonata*, are shown schematically in Figure 8. Based on the morphological changes in the cells, the entire process can be divided into the following three stages: (I) the emergence of directional (polarized) cell growth, the sign of which are dome-like and conical protrusions of transverse walls in cells adjacent to the defective and dead cells (marked in red); (II) convergence and adjacency of previously unconnected cells that carry out directional growth; (III) completion of the 'wound healing' process, i.e. restoration of the filament integrity through the formation of intercellular junction or cell fusion. The scheme demonstrates that, at the initial stage, a rupture may occur at the site of the algal filament with defective or dead cells, dividing this filament into two fragments, one of which would remain attached, and the other would be free (dashed arrow). Moreover, the scheme reflects that, in rare cases at the first stage, defective cells can restore their vital functions themselves and, hence, carry out the 'wound healing' process with subsequent mitotic division and formation of a lateral filament (dashed arrow). At the last third stage of the 'wound healing' process in *U. zonata*, two scenarios are employed through directional growth, and in both cases, the lesions are eliminated by filling the spaces of defective or dead cells with live cells. Furthermore,

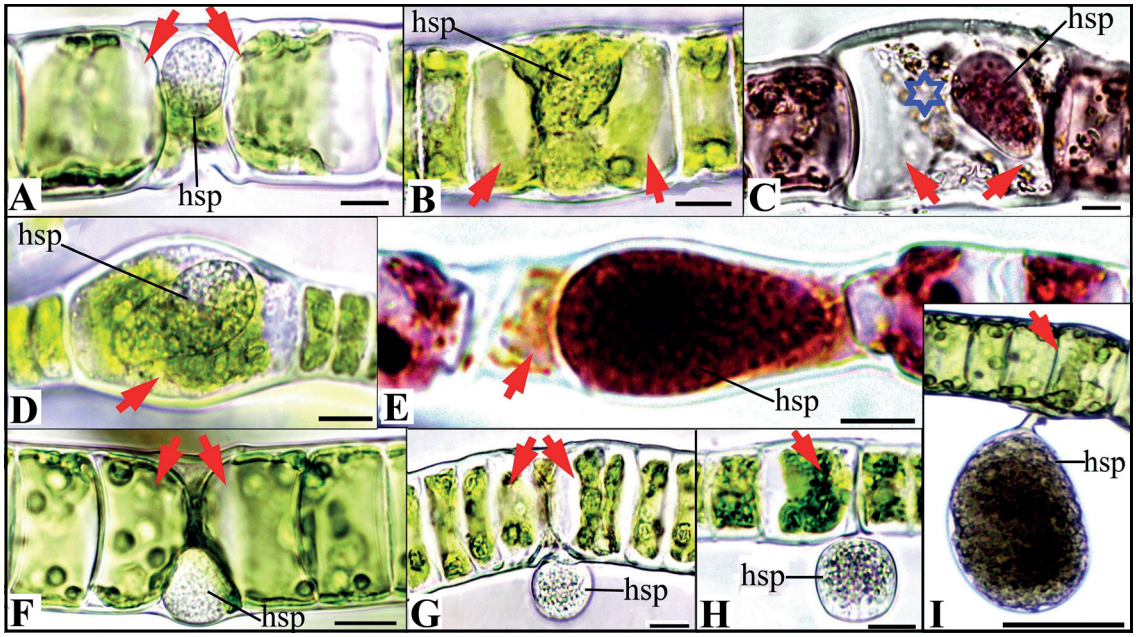

Fig.7. Development of giant hypnospores caused by the 'wound healing' process in *U. zonata*. The red arrows indicate (A) two vegetative cells that carry out directional growth to each other into the adjacent cell with a developing hypnospore (B, C) two vegetative cells in different phases of fusion during the directional to each other into the space of the adjacent cell with a developing hypnospore (the asterisk marks the area of dissolution of cell walls (C)), (D) giant cell with growing hypnospore (after completion of the fusion of two vegetative cells), (E) giant cell, inside which a giant hypnospore has developed, (F, G) vegetative cells displacing the hypnospore during their directional growth, (H) large vegetative cell that has formed after the fusion of typical vegetative cells during their directional growth and displacement of the growing hypnospore beyond the filament, and (I) intercellular septa formed by typical vegetative cells during their directional growth and displacement of the growing hypnospore beyond the filament. Designations: hsp – hypnospore. Photomicrographs of live specimens (A, B, D, and F–I) and photomicrographs of specimens with in vivo staining with acetoorcein (C, E). Scale bars: 10 μ (A–D and F–H) and 50 μ (E, I).

cell fusion leads to the emergence of a giant polyploid vegetative cell, the mitotic division of which contributes to an increase in the diameter of the filament. The scheme shows the fate of the cell and the hypnospore developing in it, which were under the pressure of the directional growth of adjacent cells. Transformations in such a cell are similar to those that occur in typical defective or dead cells during the 'wound healing' process. There are two pathways of development of the hypnospore: either inside the fused cells or beyond the filament after being displaced by cells that grow towards each other. Both cases lead to its development to a gigantic size (up to 100 μm in diameter).

The intensive development of *U. zonata* in flowing waters and surf zones of water bodies suggests that the 'wound healing' process preventing rupture of its filaments occurs rather quickly. Perhaps, its duration is the same as in the red algae, *Griffithsia pacifica* Kylin 1925, the experiments on which revealed that the repair of the filament at the site of the damaged cell occured within 24 to 30 hours (Waaland and Cleland, 1974).

The presented cytomorphological description of the 'wound healing' process in the *U. zonata* green filamentous algae had some common features with those in red algae (Lewis, 1909; Waaland and Cleland, 1974; Kim et al., 1988; Kim and Fritz, 1993). In the latter, three fundamentally different stages of this process were distinguished (Kim and Fritz, 1993). At the same time, the study of 16 species of red algae revealed three types of 'wound healing' scenarios: the fusion type detected in 13 species, the non-fusion type identified only in one species and the elongation type found in two species (Kim et al., 1988). In the first two scenarios, new (repairing) cells in the algal filaments grew towards each other from the transverse walls of the cells adjacent to the damage into the lumen of the dead cell. After adjoining each other, they mostly fusioned into a single typical shoot cell, and, in rarer cases, they formed intercellular junctions, retaining their individuality. Thus, in the vast majority of the studied species, dead cell in the filament was replaced by one cell, and only in one species – by several cells. Similar phenomena but without the formation of 'repairing' cells and involving adjacent cells themselves to the damage site also occurred in the *U. zonata* filaments, which the description, figures (Figs. 4, 5) and the scheme (Fig. 8, stage III) above reflect. In the elongation type scenario, the cells adjacent to the wound elongated, growing into the lumen of the dead cell. When they adjoined, they formed a 'pit connection' (Hawkins, 1972; Kim et al., 1988). Based on our description of the 'wound healing' process in *U. zonata*, this scenario takes place in its filaments (Figs. 3, 4, 8 (stage III)). Another cytological similarity of the 'wound healing' process between *U. zonata* and marine filamentous red algae is that during the fusion of mononuclear cells in the red algae, *Antithamnion nipponicum* Yamada et Inagaki, in the process of 'wound healing', nuclei also fusioned with an increase in their ploidity level, corresponding to an increase in cell volume (Kim et al., 1995). In other words, our hypothesis about the polyploid status of giant cells in *U. zonata* filaments formed during the

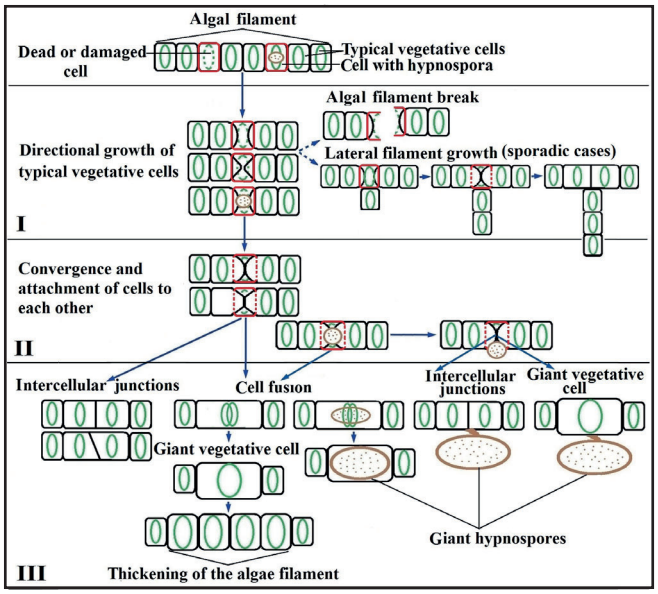

Fig.8. Three stages of the 'wound healing' process in the green filamentous algae, *U. zonata*. At stage I, signs of directional (polarized) growth appear, namely, dome-like and conical protrusions of the transverse walls in cells associated with dead and defective cells as well as with cells containing hypnospores (marked in red). During this stage, a defective cell may be restored with the development of a lateral filament from it, and also the filament may fragment at sites with dead and defective cells (dashed arrows). At stage II, the cells that carry out oppositely directional growth into the space of dead, defective and hypnospore-containing cells converge and attach to each other. Stage III is the completion of the 'wound healing' process through the formation of intercellular junctions, or through intercellular fusions. The latter leads to the emergence of giant (polyploid) vegetative cells, whose further mitotic divisions cause thickening of the original filament. The development of hypnospores during this process occurs both inside the giant cells and outside the filament. In both cases, they can grow to gigantic sizes (up to 100 μm in diameter). Green ovals are chloroplasts.

fusion of two cells in the process of 'wound healing' can be considered correct because it is consistent with previous data on other filamentous algae. The fusion of somatic cells as one of the polyploidy mechanisms was established already in the second half of the past century in both plants and animals (Brodsky and Uryvaeva, 1981; Anatskaya and Vinogradov, 2022). Polyploid plants have larger sizes of the body itself and individual organs (e.g. fruits and seeds) as well as greater resistance to adverse effects. Therefore, the formation of giant polyploidy cells in the *U. zonata* filaments not only ensures the repair of thalli but also contributes to an increase in the thickness of the filaments, thereby enhancing the viability of this species.

The nuclear dynamic movement to proper positioning at the correct functional location is essential for cellular functions in animal, fungal, and plant cells (Gundersen and Worman, 2013; Klimenkov et al., 2018; Wada, 2018). In particular, nuclear migration is required in apical, directionally growing cells to maintain a constant distance between the cell tip and the nucleus, probably to maintain an efficient supply of mRNAs necessary for tip growth and the

formation of new chloroplasts and other organelles (Baluska et al., 2003). At the first stage of 'wound healing' in filamentous red algae, the nuclei migrated to the transverse cell walls adjacent to the dead cell (Kim et al., 1995). Their mitotic division occurred there, after which, from the outer side of these walls, new 'repairing' cells replacing it began to grow into the inside of the dead cell. In *U. zonata*, we did not identify the migration of nuclei into the polarized sites of cells either during their directional growth (Fig. 2G) or during their convergence and close interaction (Fig. 3C, 3J). The convergence and fusion of nuclei in *U. zonata* occurred only after the fusion of protoplasts of two cells that converged and came into interaction (Fig. 5E–5G). Thus, the fixed position of nuclei in directionally growing cells, which we identified, indicates that they are probably somehow fixed in the protoplast. Perhaps, like in green filamentous algae of the genus *Spirogira* Link., 1820 (Fowke and Pickett-Heaps, 1969), thin cytoplasmic strands hold *U. zonata* cell nuclei in the cells centre. The German researchers H. Sawitzky and F. Grolig (1995), called these strands visible under a light microscope the nucleus positioning scaffold or NPS. In the central region of *U. zonata* cells where the nucleus is located, the chloroplast also is located in the form of a girdle. This may be the reason why such strands are difficult to detect.

Other researchers also revealed during cultivation the cases of branching in the species of the genus *Ulothrix*, including *U. zonata*, which are not typical of the common filamentous algae (Lokhorst and Vroman, 1972; 1974a; 1974b; Floyd et al., 1972; Lokhorst, 1985). The list of taxonomic features of *U. zonata* may also include the following property: «In culture, this alga show branching» (Lokhorst, 1985). Notably, all these researchers only stated this fact without providing detailed descriptions. Our study demonstrates, firstly, that branching also occasionally occurs in natural specimens and, secondly, one of the likely cytological mechanisms of the lateral filament development during 'wound healing'.

In the publication of English algologists (Jane and Woodheat, 1941), we also saw the patterns of directional growth of cells in *U. zonata* and another species of filamentous algae, *Hormidium* ref. *flaccidum* (Küntz) (this name is currently regarded a synonym of *Klebsormidium flaccidum* (Kützing) P.C.Silva, K.R.Mattox & W.H.Blackwell), which testified to the 'wound healing' process. However, this publication states the formation of H-shaped structures or thickenings in the walls of vegetative cells that, as noted by the authors, were previously described in the species of the genus *Microspora* as well as in other Ulothrix species due to the development of aplano- and macrozoospores (Fig. 9A, 9B marked in yellow). According to the opinion of F.W. Jane and N. Woodheat (1941), such thickenings appeared in algal filaments from exposure to cold because the samples were collected in the winter. Histochemical tests conducted in their study revealed that the H-shaped thickenings were the products of the outer cell walls. We believe that these H-shaped structures in algal filaments are rather sporangia without spores or former defective and dead cells that were found in winter samples of the *U. zonata* and *H. flaccidum* filaments than thickened outer cells. Figures from that publication clearly show the characteristic protrusions of the transverse walls of adjacent cells into these H-shaped structures that, in fact, are former deformed cells (Fig. 9A, 9B, red arrows). In other words, reproductive transformation or the death of cells in the filaments caused directional growth of their adjacent cells with the corresponding morphological changes. In Figures 2 and 3, the *Ulothrix* filaments are located horizontally. However, if they are turned vertically, it would be seen that the cells, into which the directional growth of adjacent cells is carried out, are deformed and H-shaped. H-shape results from the compression of defective and dead cells on the two sides by the growing adjacent cells. The authors of the indicated publication also stated that at the sites of H-shaped thickenings of the species *H. flaccidum* the filaments often ruptured, while in *U. zonata*, these H-shaped structures did not cause the fragmentation of the filaments. Therefore, in *U. zonata*, the sites of filaments where the 'wound healing' process has begun can be rather resistant to rupture. Our observation that retained sheaths of dead cells contribute to the thickening of the intercellular walls of vegetative cells (Fig. 4H) corresponds to the results in F.W. Jane and N. Woodhead (1941). Perhaps, thanks to this publication, H-shaped structures or septa (or the remains of dead cells, as we define them) were taken into account during taxonomic descriptions of the Ulothrix algae (Lokhorst and Vroman, 1972; 1974a; 1974b; Floyd et al., 1972; Lokhorst, 1985). For example, the morphological characterization of cultivated specimens of *U. zonata* indicated that «H-pieces may be present in all filamentous stages, but are more common in older cultures» (Lokhorst and Vroman, 1974b). Similar situations were observed in the cultivation of other species of the genus *Ulothrix* (Lokhorst and Vroman, 1974a). This confirms our conclusion about the formation of H-shaped septa from

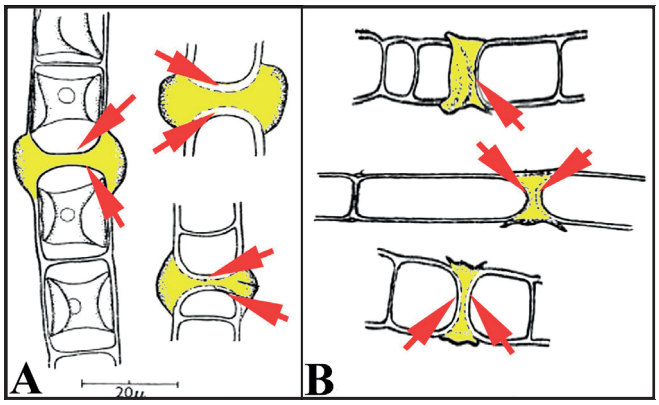

Fig.9. H-shaped structures in the walls of *U. zonata* (A) and *Hormidium* ref. *flaccidum* (Küntz) (B) (according to F.W. Jane and N. Woodheat, 1941). H-shaped structures (former defective and dead cells, according to our definition) are marked in yellow, and arrows indicate the protrusions of transverse cell walls that carry out growth towards each other.

the sheaths of dead cells: in old (depleted) cultures, cell death rate was naturally higher than in other cultures.

Image of giant vegetative cells that underwent divisions in the species of green filamentous algae, *Rhizoclonium subtile* Z. Zhao & G. Liu, sp. nov., was presented in the article on the phylogenetic analysis of the genus *Rhizoclonium* Kützing, 1843 (Cladophoraceae, Cladophorales) from China (Zhao et al., 2018). The authors called them 'swollen cells' without explaining their origin. As seen in our description, in *U. zonata*, these 'swollen cells', i.e. giant cells, resulted from cell fusion during directional growth. Moreover, in this publication, photomicrographs of this algae clearly showed dome-like protrusions of transverse cells in some cells directed into the empty spaces of filaments towards each other where dead cells were likely located. Also, cells of an atypical cylindric shape are also visible in the filaments, indicating contact and subsequent cell fusion during growth towards each other (Zhao et al., 2018). According to modern taxonomy (Algae Base, https://www.algaebase.org/), the genera *Rhizoclonium* and *Ulothrix*, belong to the same class of green algae, Ulvophyceae. This probably determines the existence of similar cytological mechanisms in *U. zonata* and *R. subtile*, in particular, the 'wound healing' process.

According to modern taxonomy (Algae Base, https://www.algaebase.org/), the above-mentioned taxa, which, in our opinion, have characteristic features of "wound healing", represent three phyla (types) and four families of filamentous algae. Two species, *U. zonata* (***Family*** Ulotrichaceae) and *Rhizoclonium subtile* (***Family*** Cladophoraceae), represent the Phylum Clorophyta, the green filamentous algae. The species *H. flaccidum* or *Klebsormidium flaccidum* (***Family*** Klebsormidiaceae) belongs to the ***Phylum*** Charophyta, charophytes. The marine red algae, *G. pacifica* (***Family*** Wrangeliaceae), are members of the ***Phylum*** Rhodophyta, a type of red algae. Based on this information about the occurrence of repair in different taxonomic groups, as well as from our study, we conclude that the 'wound healing' process due to cell growth towards each other with their subsequent fusion or connection is a natural biological property of the species *U. zonata* and possibly is also present in natural populations of other filamentous algae. Cytological patterns that we described, as well as H-shaped intercellular septa in filaments detected previously (Jane and Woodheat, 1941), are markers of both this process and its preceding abnormalities and death of cells. Thus, the frequency of the 'wound healing' processes in the prepared filaments can also indicate the degree of damage to the algal thalli. For instance, microscopy of the studied *U. zonata* specimens revealed that they can be divided into two groups that dramatically differ in the number of cases of filament repair in one cytological preparation. The first group with a low occurrence of the 'wound healing' episodes included the samples collected in Lake Baikal opposite the Kultuk and Marituy settlements as well as near the Katorzhanka River (brook 1.5 m wide and 15 cm deep) (Fig. 10A). From 20 to 50 episodes of filament repair could be observed in one cytological preparation (S = 7.5 cm^2) of the *U. zonata* thalli from these sites. The second group included the *U. zonata* specimens with a high occurrence of 'wound healing', which were collected near Polovinny Cape (Lake Baikal, estuary of the Bolshaya Polovinnaya River), in the Zhilishche River, the Angara River: the Angara source, downstream of the Irkutsk Hydroelectric Power Station and one of its coves, as well as in the Ida River (the Angara tributary) (Fig. 10B–10D). In these samples, 1000 or more above-described patterns of different stages of 'wound healing' could be counted in one cytological preparation (with the same area: S = 7.5 cm^2). In other words, in each field of vision of the microscope at 100x magnification, there were ten or more cases of filament reparation. Furthermore, in such samples, individual filaments might also have many sites with 'wound healing' (Fig. 10C, 10D). Therefore, algal thalli had a higher degree of damage in rivers and their estuaries than in the lake.

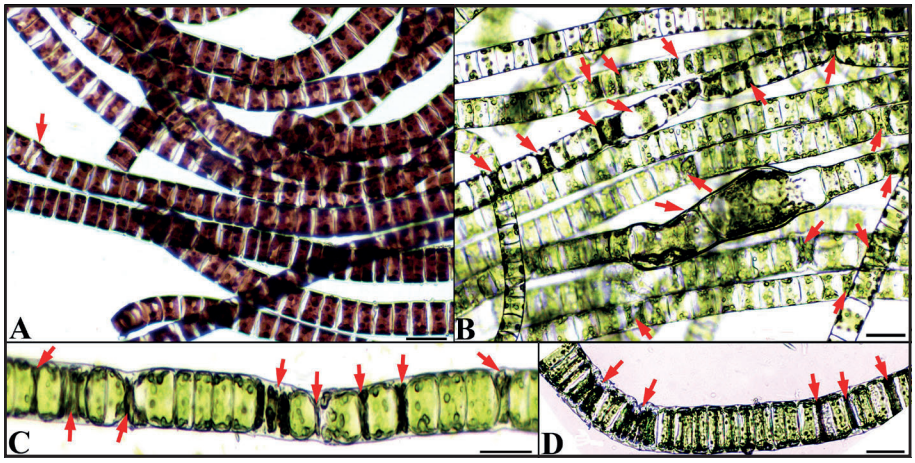

Fig.10. Low (A) and high (B) frequency of the 'wound healing' episodes (indicated by arrows) in the thalli of the filamentous algae, *U. zonata*. Samples collected in Lake Baikal opposite the Kultuk settlement (A) and in the source of the Angara River from a 5 m depth (B). Individual filaments with numerous 'wound healing' episodes (indicated by arrows) from the samples collected in the Angara (downstream of the Irkutsk Hydroelectric Power Station) (C) and Zhilishche (D) rivers. Photomicrographs of filaments stained with vivo in acetoorceine (A) and photomicrographs of live filaments (B–D). Scale bar: 50 μ.

Based on modern concepts, directional growth (polarized growth or tropism) in plants is associated with a redistribution of auxin phytohormones in cells (Blum et al., 2012; Kuluev and Safiullina, 2015). The root meristem of the known model plant, *Arabidopsis thaliana* (L) Heynh, revealed that activation of auxin production in its surrounding cells was one of the most substantial responses to damage (Hoermayer and Friml, 2019). This phytohormone plays a key role not only in the processes of growth and development of plants but also in the restoration of tissues and organs. To date, it has been also shown that phytohormones play an important role in the vital activity of algae, and green algae (Chlorophyta) are one of the taxonomic groups where their greatest number has been characterised (Tarakhovskaya et al., 2007; Kiseleva et al., 2012). In particular, the studied spectrum of auxin action in macroalgae vegetation indicated its role in growth regulation (thallus branching and rhizoid formation) and formation of reproductive structures, which corresponds to the functions of phytohormones in higher plants. In the red filamentous algae, *G. pacifica*, during the rupture of the filament in the basal cell of one of the fragments, the rhodomorphin phytohormone is released, under the influence of which the apical cell of the second fragment forms a specific 'repairing' cell that ensures cell fusion and restoration of filaments (Waaland and Watson, 1980). Other biologically active substances can also play an important role in the regulation of the 'wound healing' process in algae. The species *U. zonata* descdibed in our study is an easily accessible model object to search for these components and determine their role in biochemistry of the repair process.

4. Conclusions

For more than two hundred years of studies of the *U. zonata* green filamentous algae, we have revealed and described for the first time a cytomorphological pattern of self-healing (repair) of damaged filament sites (with defective and dead cells), which is called 'wound healing' in scientific literature, including algological literature. Moreover, for the first time in the field of algology, we have studied this process in the samples collected from natural populations. In this regard, we think that the following fact is of interest. To date, due to the lack of information on repair of macroalgae filaments in natural conditions, some researchers have concluded that such an adaptation cannot appear in them in the course of evolution. In other words, these researcher believe that only rupture and fragmentation of filaments (water immediately separates fragments from each other) occur due to cell damage in algae under natural aquatic conditions; therefore, in thei opinion, algae could not develop a 'wound healing' mechanism. For example, the 'wound healing' process that occurred in the experiment with red filamentous algae, according to one of these researchers, can be considered a model of cell intelligence (Ford, 2010; 2017). They stated that cells in an unpredictable situation were able to 'guess' how to act correctly, 'turning on' a genetically unprogrammed mechanism. Brian J. Ford (2017, caption to Fig. 11) wrote about this: "Within thirty hours, the damaged cell has been restored in its entirety and is functioning as before. Since this is an unprecedented eventuality for which the cells invoke remedial action, it has clear connotations of intelligent behavior." Our and other studies have revealed that restoration of thalli in algae through directional cell growth is a rather widespread phenomenon in their natural population, which is very important: to ensure the preservation of vital activity of individuals (i.e. filaments), which works not only in artificial but also in natural conditions. In this regard, 'wound healing' is an evolutionary developed cytological mechanism encoded in cell genomes. Furthermore, as our study indicates, directional cell growth is carried out not only into defective but also into live cells with developing hypnospores, reproductive structures, in which thousands of spores mature, giving rise to new filaments. Sometimes, in the course of such growth, hypnospores are even displaced beyond the filaments where their development can be complicated or stopped. In these cases, deirectionally growing cells suppresses the reproduction process, that is unreasonable in terms of species development. However, in the course of evolution of the species *U. zonata*, the 'wound healing' process with its pressure of directional cell growth, on the contrary, has developed to contribute to the formation of giant hypnospores. This adaptation increases the reproductive abilities of *U. zonata* and contributes to its successful dispersal throughout the globe.

The natural phenomenon of somatic cell fusion in the representative of the lower plants, the *U. zonata* filamentous algae, revealed in our study can serve as a convenient model for studying its mechanism because the information about it is limited.

The various revealed deformations of typical vegetative cells in the studied samples indicate that 'wound healing' in these filamentous algae is the process of a successive alteration of the characteristic morphological transformations of the cell walls, based on which we can determine the stages of filament restoration. A comparison of our data with the results of other studies has revealed that the cytological patterns of filament repair in *U. zonata* have some similarities and differences with those in marine red filamentous macroalgae. Moreover, substances accompanying the 'wound healing' process in marine algae appeared to be attractive for medical purposes (Kuznetsova et al., 2020). Therefore, we believe that further study of this significant self-healing ability in this typical and widespread representative of aquatic vegetation may also be promising.

Acknowledgments

This research was funded by the Russian State Project No. 0279-2022-0010

We are greaful to the reviewer for his careful reading of our manuscript and very helpful comments.

Special thanks to the crew of the research vessel "Titov" for their help in collecting samples.

We thank Dr. A. P. Fedotov for collecting bottom samples of *U. zonata* from Lake Baikal near Listvyanka settlement

We are very grateful to Dr. L.S. Kravtsova for important explanations and comments in the course of our work.

We thank Dr. N. A. Bondarenko for her helpful consultation.

Conflict of interests

The authors declare no conflict of interests.

References

Anatskaya O.V., Vinogradov A.E. 2022. Polyploidy as a fundamental phenomenon in evolution, development, adaptation and diseases. International Journal of Molecular Sciences 23(7): 3542. DOI: 10.3390/ijms23073542

Baluska F., Wojtaszek P., Volkmann D. et al. 2003. The architecture of polarized cell growth: the unique status of elongating plant cells. Bioessays 25: 569-576. DOI: 10.1002/bies.10282

Blum Ya.B., Krasylenko Yu.A., Emets A.I. 2012. Effect of phytohormones on the cytoskeleton of the plant cell. Russian Journal of Plant Physiology 59: 515-529. DOI: 10.1134/S1021443712040036

Bondarenko N.A., Obolkina L.A., Melnik N.G. 2009. Cryobiology of Lake Baikal: state-of-the-art and main trends of research. In: Timoshkin O.A., Proviz V.I., Sitnikova T.Ya et al. (Eds.), Index of animal species inhabiting Lake Baikal and its catchment area: In 2 volumes. Vol. II: Basins and channels in the south of East Siberia and North Mongolia. Book 1: Guides and keys to identification of fauna and flora of Lake Baikal. Novosibirsk: Nauka.

Brodsky V.Y., Uryvaeva I.V. 1981. Kletochnaya poliploidiya. Proliferatsiya i differentsirovka [Cellular polyploidy. Proliferation and differentiation]. Moskow: Nauka. (in Russian)

Brown R.C., Lemmon B.E. 2001. The cytoskeleton and spatial control of cytokinesis in the plant life cycle. Protoplasma 215: 35-49. DOI: 10.1007/BF01280302

Bullock K.W. 1978. Observations on hypnospores in *Ulothrix zonata* (Chlorophyceae). Canadian Journal of Botany 56(14): 1660-1664. DOI: 10.1139/b78-196

Burr F.A., West J.A. 1972. A cytochemical study of the wound-healing protein in *Bryopsis hypnoides*. Cytobios 6: 199-215.

Cells. 2007. In: Lewin B., Cassimeris L., Lingappa V. et al. (Eds.). Sudbury, MA: Jones and Bartlett Publishers.

Cole R.A., Fowler J.E. 2006. Polarized growth: maintaining focus on the tip. Current Opinion in Plant Biology 9(6): 579-588. DOI: 10.1016/j.pbi.2006.09.014

Colombo P.M., De Carli M.E. 1980. Morphological and ultrastructural aspects of regeneration following wounding in the *Udotea petiolata* thallus. Cytobios 27(107-108): 147-155.

Dingman J.E., Lawrence J.E. 2012. Heat-stress-induced programmed cell death in *Heterosigma akashiwo* (Raphidophyceae). Harmful Algae 16: 108-116. DOI: 10.1016/j.hal.2012.02.003

Ehlers K., Kollmann R. 2001. Primary and secondary plasmodesmata: structure, origin, and functioning. Protoplasma 216(1): 1-30. DOI: 10.1007/BF02680127

Esmon C.A., Pedmale U.V., Liscum E. 2005. Plant tropisms: providing the power of movement to a sessile organism. The International Journal of Developmental Biology 49: 665-674. DOI: 10.1387/ijdb.052028ce

Floyd G.L., Stewart K.D., Mattox K.R. 1972. Comparative cytology of *Ulothrix* and *Stigeoclonium*. Journal of Phycology 8: 68-81. DOI: 10.1111/j.1529-8817.1972.tb04004.x

Foissner I. 1988. The relationship of echinate inclusions and coated vesicles on wound healing in *Nitella flexilis* (Characeae). Protoplasma 142(2-3): 164-175. DOI: 10.1007/BF01290873

Foissner I., Wasteneys G.O. 1997. A cytochalasin-sensitive actin filament meshwork is a prerequisite for local wound wall deposition in *Nitella internodal* cells. Protoplasma 200: 17-30. DOI: 10.1007/BF01280731

Ford B.J. 2010. A new era for whole cell biology. Biologist 57(1): 9-11. URL: http://www.brianjford.com/a-10-biol-cell.pdf

Ford B.J. 2017. Cellular intelligence: microphenomenology and the realities of being. Progress in Biophysics and Molecular Biology 131: 273-281. DOI: 10.1016/j.pbiomolbio.2017.08.012

Fowke L.C., Pickett-Heaps J.D. 1969. Cell division in *Spirogyra*. I. Mitosis. Journal of Phycology 5(3): 240-259. DOI: 10.1111/j.1529-8817.1969.tb02609.x

Gachon C.M.M., Sime-Ngando T., Strittmatter M. et al. 2010. Algal diseases: spotlight on a black box. Trends in Plant Science 15(10): 633-640. DOI: 10.1016/j.tplants.2010.08.005

Garbary D.J., Galway M.E., Lord C.E. et al. 2012. Programmed cell death in multicellular algae. In: Heimann K., Katsaros C. (Eds.), Advances in algal cell biology. Berlin, Boston: De Gruyter, pp. 1-20. DOI: 10.1515/9783110229615.1

Girloy S. 2008. Plant tropisms. Current Biology 18(7): 275-277. DOI: 10.1016/j.cub.2008.02.033/

Gundersen G.G., Worman H.J. 2013. Nuclear positioning. Cell 152(6): 1376-1389. DOI: 10.1016/j.cell.2013.02.031

Hawkins E.K. 1972. Observations on the developmental morphology and fine structure of pit connections in red algae. Cytologia 37: 759-768. DOI: 10.1508/cytologia.37.759

Hoermayer L., Friml J. 2019. Targeted cell ablation-based insights into wound healing and restorative patterning. Current Opinion in Plant Biology 52: 124-130. DOI: 10.1016/j.pbi.2019.08.006

Höfler K. 1934. Regenerationsvorgänge bei *Griffithsia schousboei* [Regenerative processes in *Griffithsia schousboei*]. Flora 27: 331-344. DOI: 10.1016/S0367-1615(17)31813-X (in German)

Izhboldina L.A. 2007. Atlas i opredelitel' vodorosley bentosa i perifitona ozera Baikal (meyo- i makrofity) s kratkimi ocherkami po ikh ekologii [Atlas and key to benthic and periphyton of Lake Baikal (meyo- and macrophytes) with short essays on their ecology]. Novosibirsk: Science Center. (in Russian)

Jaffar M.Z.A.M, Davidson F.A. 2013. Basic rules for polarised cell growth. Journal of Theoretical Biology 336(7): 44-51. DOI: 10.1016/j.jtbi.2013.06.039

Janczewski E. 1876. Notes sur le développement du cystocarpe dans les Floridées. Mém. Soc. nat des Sciences Nat. de Cherbourg. 1876(7): 109-44. (in French)

Jane F.W., Woodhead N. 1941. The formation of "H-Pieces" in the walls of *Ulothrix* and *Hormidium*. The New Phytologist 40(3): 183-188. URL: http://www.jstor.org/stable/2428983

Jarvis M.C., Briggs S.P.H., Knox J.P. 2003. Intercellular adhesion and cell separation in plants. Plant, Cell and Environment 26: 977-989. DOI: 10.1046/j.1365-3040.2003.01034.x

Kim G.H., Fritz L. 1993. A signal glycoprotein with a-d-mannosyl residues is involved in the wound-healing response of *Antithamnion sparsum* (Ceramiales, Rhodophyta). Journal of Phycology 29: 85-90. DOI: 10.1111/j.1529-8817.1993.tb00284.x

Kim G.H., Klotchkova T.A., Kang Y.M. 2001. Life without a cell membrane: regeneration of protoplasts from disintegrated cells of the marine green alga *Bryopsis plumosa*. Journal of Cell Science 114: 2009-2014. DOI: 10.1242/jcs.114.11.2009

Kim G.H., Lee I.K., Fritz L. 1995. The wound-healing responses of *Antithamnion nipponicum* and *Griffitsia pacifica* (Ceramiales, Rhodophyta) by lectins. Phycological Research 43: 161-166. DOI: 10.1111/j.1440-1835.1995.tb00020.x

Kim H.S., Kim G.H., Lee I.K. 1988. Wound-healing in several filamentous red algae, Ceramiales. The Korean Journal of Phycology 3(1): 15-27. URL: https://www.researchgate.net/profile/Gwang-Hoon-Kim/publication/263929575_Wound_healing_m_several_filamentous_red_algae_Ceramiales/links/0deec53c64a4dcdb6c000000/Wound-healing-m-several-filamentous-red-algae-Ceramiales.pdf

Kiseleva A.A., Tarachovskaya E.R., Shishova M.F. 2012. Biosynthesis of phytohormones in algae. Russian Journal of Plant Physiology 59(5): 595-610. DOI: 10.1134/S1021443712050081

Klimenkov I.V., Sudakov N.P., Pastukhov M.V. et al. 2018. Rearrangement of actin microfilaments in the development of olfactory receptor cells in fish. Scientific Reports 8(1): 1-12. DOI: 10.1038/s41598-018-22049-7

Kravets E.A. 2008. Cell competition in vegetative and generative meristems and its role in recovery mechanisms under irradiation. Faktory Eksperimental'noy Evolyutsii Organizmov [Factors of Experimental Evolution of Organisms] 4: 86-90. (in Russian)

Kravtsova L.C., Izhboldina L.A., Khanaev I.V. et al. 2014. Nearshore benthic blooms of filamentous green algae in Lake Baikal. Journal of Great Lakes Research 40: 441-448. DOI: 10.1016/j.jglr.2014.02.019

Kuluev B.R., Safiullina M.G. 2015. Regulation of cell expansion in plants. Uspekhi Sovremennoi Biologii [Advances in Modern Biology] 135(2): 148-163. (in Russian)

Kützing F.T. 1833. Algologische Mittheilungen II. Ueber eine neue Gattung der Confervaceen. Flora 16(35): 513-521. (in German)

Kuznetsova T.A., Andryukov B.G., Besednova N.N. et al. 2020. Marine algae polysaccharides as basis for wound dressings, drug delivery, and tissue engineering: a review. Journal of Marine Science and Engineering 8(7): 481. DOI: 10.3390/jmse8070481

La Claire J.W. 1982. Cytomorphological aspects of wound healing in selected Siphonocladales. Journal of Phycology 18: 379-384. DOI: 10.1111/j.1529-8817.1982.tb03199.x

La Cour L. 1941. Acetic-orcein: a new stain-fixative for chromosomes. Stain Technology 16(4): 169-174. DOI: 10.3109/10520294109107302

Lewis I.F. 1909. The life history of *Griffithsia bornetiana*. Annals of Botany 23(4): 639-690. DOI: 10.1093/oxfordjournals.aob.a089246

Lokhorst G.M. 1985. The concept of the genus *Ulothrix* (Chlorophyta) strengthened by comparative cytology. Biosystems 18(3-4): 357-368. DOI: 10.1016/0303-2647(85)90035-8

Lokhorst G.M. Vroman M. 1972. Taxonomic study on three freshwater *Ulothrix* species. Acta Botanica Neerlandica 21(5): 449-480. URL: https://www.natuurtijdschriften.nl/pub/539866

Lokhorst G.M., Vroman M. 1974a. Taxonomic studies on the genus *Ulothrix* (Ulotrichales, chlorophyceae). II. Acta Botanica Neerlandica 23(4): 369-398. DOI: 10.1111/j.1438-8677.1974.tb00957.x

Lokhorst G.M., Vroman M. 1974b. Taxonomic studies on the genus *Ulothrix* (Ulotrichales, Chlorophyceae) III. Acta Botanica Neerlandica 23(5/6): 561-602. DOI: 10.1111/j.1438-8677.1974.tb00971.x

Maruyama D., Ohtsu M., Higashiyama T. 2016. Cell fusion and nuclear fusion in plants. Seminars in Cell and Developmental Biology 60: 127-135. DOI: 10.1016/j.semcdb.2016.07.024

Menzel D. 1988. How do giant plant cells cope with injury? – the wound response in siphonous green algae. Protoplasma 144: 73-91. DOI: 10.1007/BF01637240

Meyer K.I. 1930. Introduction to algal flora of Lake Baikal. Byulleten' Moskovskogo Obshchestva Ispytateley Prirody. Otdel Biologicheskiy [Bulletin of Moscow Society of Naturalists. Biological series] 39: 179-392. (in Russian)

Mine I., Menzel D., Okuda K. 2008. Morphogenesis in giant-celled algae. International Review of Cell and Molecular Biology 266: 37-83. DOI: 10.1016/S1937-6448(07)66002-X

Mironova V., Xu J. 2019. A single-cell view of tissue regeneration in plants. Current Opinion in Plant Biology 52: 149-154. DOI: 10.1016/j.pbi.2019.09.003

Moshkova N.A., Gollerbakh M.M. 1986. Opredelitel' presnovodnykh vodorosley SSSR. Zelenyye vodorosli. Klass ulotriksovyye (1). [Keys to freshwater algae of the USSR. Green algae. Ulotrix Class (1)]. Leningrad: Nauka. (in Russian)

Nguyen S.T.T., McCurdy D.W. 2016. Transdifferentiation – a plant perspective. In: Rose R.J. (Ed.), Molecular cell biology of the growth and differentiation of plant cells. Boca Raton, Florida: CRC press.

Nichols S.P. 1922. Methods of healing in some algal cells. American Journal of Botany 9: 18-29. DOI: 10.1002/j.1537-2197.1922.tb05648.x

Obroucheva N.V. 2008. Cell elongation as an inseparable component of growth in terrestrial plants. Russian Journal of Developmental Biology 39(1): 13-24. DOI: 10.1134/S1062360408010049

Pausheva Z.P. 1988. Praktikum po citologii rasteniy [Workshop on plant cytology]. Moscow: Agropromizdat. (in Russian) URL: https://www.studmed.ru/view/pausheva-zp-praktikum-po-citologii-rasteniy_3d3076b33d8.html

Polevoy V.V. 1998. Ways of plant movement. Sorosovskiy Obrazovatel'nyy Zhurnal [Soros Educational Journal] 1: 21-27. (in Russian) URL: https://web.archive.org/web/20070818144246/http://journal.issep.rssi.ru/author.php?author=451

Sawitzky H., Grolig F. 1995. Phragmoplast of the green alga *Spirogyra* is functionally distinct from the higher plant phragmoplast. The Journal of Cell Biology 130(6): 1359-137. DOI: 10.1083/jcb.130.6.1359

Shyam R., Saxena P.N. 1980. Morphological and cytological investigations of *Ulothrix zonata* and taxonomy of the related species. Plant Systematics and Evolution 135: 151-158. DOI: 10.1007/BF00983183

South G.R., Whittick A. 1990. Osnovy al'gologii [Introduction to phycology]. Moscow: Mir. (in Russian)

Starmach K. 1972. Flora slodkowodna Polski: Chlorophyta III. Zielenice nitkowate [Freshwater flora of Poland: Chlorophyta III. Filamentous green algae]. Polska Akademia Nauk, Instytut Botaniki, Krakow. (in Polish)

Sugiyama M. 2015. Historical review of research on plant cell dedifferentiation. Journal of Plant Research 128: 349-359. DOI: 10.1007/s10265-015-0706-y

Tarakhovskaya E.R., Maslov Y.I., Shishova M.F. 2007. Phytohormones in algae. Russian Journal of Plant Physiology 54: 163-170. DOI: 10.1134/S1021443707020021

Tatewaki M., Nagata K. 1970. Surviving protoplasts in vitro and their development in *Bryopsis*. Journal of Phycology 6: 401-403. DOI: 10.1111/j.1529-8817.1970.tb02414.x

Vasser S.P., Kondrat'eva N.V., Masyuk N.P. et al. 1989. Vodorosli. Spravochnik [Algae. Reference Book]. Kiev: Naukova Dumka. (in Russian)

Waaland S.D., Cleland R.E. 1974. Cell repair through cell fusion in the red alga *Griffithsia pacifica*. Protoplasma 79: 185-196. DOI: 10.1007/BF02055788

Waaland S.D., Watson B.A. 1980. Isolation of a cell-fusion hormone from *Griffithsia pacifica* Kylin, a red alga. Planta 149: 493-497. DOI: 10.1007/BF00385754

Wada M. 2018. Nuclear movement and positioning in plant cells. Seminars in Cell and Developmental Biology 82: 17-24. DOI: 10.1016/j.semcdb.2017.10.001

Wang P.-H.P., Huang B., Horng H.-Ch. et al. 2018.Wound healing. Journal of the Chinese Medical Association 81(2): 94-101. DOI: 10.1016/j.jcma.2017.11.002

Watson B.A., Waaland S.D. 1986. Further biochemical characterization of a cell fusion hormone from the red alga, *Griffithsia pacifica*. Plant and Cell Physiology 27(6): 1043-1050. DOI: 10.1093/oxfordjournals.pcp.a077187

Weber F., Mohr D.M.H. 1804. Naturhistorische Reise durch einen Theil Schwedens. Göttingen. (in German)

Wilkinson H.N., Hardman M.J. 2020. Wound healing: cellular mechanisms and pathological outcomes. Open Biology 10: 200-223. DOI: 10.1098/rsob.200223

Wittmann W. 1965. Aceto-iron-haematoxylin-chloral hydrate for chromosome staining. Stain Technology 40(3): 161-164. DOI: 10.3109/10520296509116398

Zhao Z.J., Zhu H., Liu G.X. et al. 2018. Phylogenetic analysis of *Rhizoclonium* (Cladophoraceae, Cladophorales), and the description of *Rhizoclonium subtile sp. nov*. from China. Phytotaxa 383(2): 147-164. DOI: 10.11646/phytotaxa.383.2.2